Ahr-bacterial diet interaction modulates aging and associated pathologies in *C. elegans*

Vanessa Brinkmann [1], Alfonso Schiavi [1,2], Anjumara Shaik [1,2], Daniel R. Puchta[1], Ralph Menzel [3], Natascia Ventura [1,2,*]

1. IUF-Leibniz Institute for environmental Medicine at the Heinrich Heine University Düsseldorf, Auf'm Hennekamp 50, 40225 Düsseldorf, Germany
2. Institute of Clinical Chemistry and Laboratory Diagnostic, Heinrich Heine University Düsseldorf, Moorenstr 5, 40225 Düsseldorf, Germany
3. Institute of Biology, Humboldt-University Berlin, Philippstr. 13, 10115 Berlin, Germany

* Correspondence: natascia.ventura@uni-duesseldorf.de

Running title: Ahr-bacteria in *C. elegans'* healthspan

Character count: 28380

Abstract

Genetic and environmental factors concurrently shape the aging process. The nematode *Caenorhabditis elegans* has been instrumental in the past 30 years to identify most factors and pathways nowadays known to modulate aging. The aryl-hydrocarbon-receptor (AhR) is a transcription factor originally discovered as a dioxin-binding protein and involved in the metabolism of different environmental toxicants and xenobiotics. Since its discovery, the variety of pathophysiological processes regulated by the AhR has grown and previously we disclosed it promotes aging phenotypes across species. Here, we followed up on our previous study and show that lack of *C. elegans* AHR-1 differentially affects health and lifespan in a context-dependent manner. Notably, we identified a critical role for AhR-bacterial diet interaction in animal lifespan, stress resistance, and age-associated pathologies, and narrowed down the dietary factor involved in the observed AhR-dependent features to a bacteria extruded product, likely derived from tryptophan metabolism.

Keywords: Aging / Aryl hydrocarbon receptor / *C. elegans* / Microbiota

Introduction

Aging affects every human and is accompanied by increased morbidity (*e.g.,* diabetes, cardiovascular diseases, neurodegenerative diseases, and cancer) and risk of death (Kaeberlein, 2016, Lopez-Otin, Blasco et al., 2013). In the past decades, also thanks to the growing number of researchers exploiting simple but powerful model organisms such as the nematode *Caenorhabditis elegans* (*C. elegans*), numerous hallmarks of aging as well as genetic and environmental factors regulating it have been identified (Dato, Rose et al., 2017, Lopez-Otin et al., 2013, Tigges, Krutmann et al., 2014).

The aryl hydrocarbon receptor (AhR) is a highly conserved transcription factor of the bHLH PAS family originally discovered as a dioxin-binding protein (Poland, Glover et al., 1976) and involved in the metabolism of different environmental toxicants and xenobiotics. Since its discovery, the variety of pathophysiological processes regulated by the AhR has grown and range from cell death, to immune response and neuronal development (Esser, Lawrence et al., 2018). Contradictory studies also indicated a role for AhR in the aging process (reviewed in (Brinkmann, Ale-Agha et al., 2020)) and more recently, pro-aging functions of AhR (Eckers, Jakob et al., 2016, Williams, Mouchiroud et al., 2014) have been described in an evolutionarily conserved manner from *C. elegans* to mammals. In mammals, in basal conditions, AhR is bound by HSP90, AIP, and p23, which retain it in the cytoplasm, in a ligand-affine state. Ligand binding of an AhR agonist leads to the dissociation of the AhR binding complex and AhR nuclear translocation (Ashida, Nishiumi et al., 2008, Ikuta, Eguchi et al., 1998). In the nucleus, AhR dimerizes with the AhR nuclear translocator (Arnt), and the AhR-Arnt heterodimer then binds to the xenobiotic responsive elements (XREs) on AhR target genes (Ashida et al., 2008). Similar to its mammalian counterpart, the *C. elegans* AhR homolog, AHR-1, forms a heterodimer with the *C. elegans* Arnt homolog AHA-1 and binds to XREs (Powell-Coffman, Bradfield et al., 1998). It is expressed in several types of neurons and plays a role in neurodevelopment and long-chain unsaturated fatty acid synthesis

(Aarnio, Storvik et al., 2010, Huang, Powell-Coffman et al., 2004, Qin & Powell-Coffman, 2004, Qin, Zhai et al., 2006, Smith, O'Brien et al., 2013). However, unlike mammalian AhR it does not bind to TCDD or β-naphthoflavone (Powell-Coffman et al., 1998), but no other modulators have been tested so far for their effect on *C. elegans* AHR-1 activity and downstream effects. Although AhR was originally discovered as a dioxin-binding protein (Poland et al., 1976) in more recent years many other compounds have been identified which modulate its activity and can be mainly divided into four categories: xenobiotics (*e.g.,* 2,3,7,8-tetrachlorodibenzodioxin (dioxin) and benzo(a)pyrene (BaP)), dietary factors (*e.g.,* kaempferol, and curcumin), endogenous modulators (*e.g.,* 6-formylindolo[3,2-b]carbazole (FICZ) and kynurenine) and ligands generated by the microbiota metabolism (*e.g.,* indole-3-acetate and tryptamine*) (Amakura, Tsutsumi et al., 2003, Fritsche, Schafer et al., 2007, Jin, Lee et al., 2014, Lee, McPherson et al., 2017, Opitz, Litzenburger et al., 2011, Poland et al., 1976, Rannug, Rannug et al., 1987, Shimizu, Nakatsuru et al., 2000)*. Interestingly, many of these AhR modulators may impact on aging and age-associated pathologies (Alavez, Vantipalli et al., 2011, Caesar, Jonson et al., 2012, Lim, Chu et al., 2001), but whether these effects are AhR-dependent and whether AhR itself influences the progression of these diseases has been largely unexplored. Here, using *C. elegans* as a powerful model organism for aging and toxicology studies, we followed up on our previous finding indicating an anti-aging effect of *C. elegans ahr-1* depletion (Eckers et al., 2016) and investigated the effect of possible AHR-1 modulators on aging and other age-related features, such as stress response and associated pathologies. Our findings indicate that *C. elegans* can be exploited to study evolutionarily conserved functions of AhR modulators and their regulated processes and therefore to contribute to the discovery of novel information about AhR in mammals. Most importantly, we identify aging and associated pathologies as novel life traits regulated by the AhR in a diet-dependent manner bringing further complexity to the landscape of AhR-microbiota regulated processes.

Results

C. elegans AHR-1 is differentially involved in stress response

Loss of AHR-1 extends *C. elegans'* health- and lifespan (Eckers et al., 2016). Here we assessed the role of *ahr-1* in different age-correlated features. Lifespan extension often correlates with increased resistance to different types of stressors (Cypser & Johnson, 2002). We assessed AhR role in stress resistance by exposing wild-type as well as *ahr-1* mutants to either heat shock, metabolic stressors (i.e. high concentrations of glucose or the hypoxia mimetic iron chelator 2,2'Bipyridyl, BP) or UVB radiations. In agreement with the literature, the development and fertility of wild-type animals were affected by all insults in a dose-dependent manner (**Figure 1**) (Rieckher, Bujarrabal et al., 2018, Schiavi, Maglioni et al., 2015). Consistent with our previous data (Eckers et al., 2016) loss of *ahr-1* increased heat-stress resistance (**Figure 1 A, B**), however, surprisingly, it did not confer resistance to any of the newly tested insults (**Figure 1 C - H**). Actually, *ahr-1(ju145)* mutants were even more sensitive to UVB radiations since their developmental delay and embryonic lethality were significantly more affected than in wild-type worms (**Figure 1 G, H**).

Mammalian AhR typically regulates the expression of phase-I and phase-II detoxification enzyme genes like *cyps* (*e.g.*, *CYP1A1* or *CYP1B1*), *ugts* (*e.g., UGT1A1* or *UGT1A6*) and *gsts* (*e.g., GSTA1* or *GSTA2*) (Ashida et al., 2008, Xue, Li et al., 2017, Yueh, Huang et al., 2003). Thus, to further characterize animals' stress response, we quantified the expression of *C. elegans* transgenic reporters for different detoxification genes in control and upon *ahr-1* RNA interference (RNAi). Out of nine tested reporters, we found five genes (*cyp-35A2*, *cyp-35B1, gst-4, cyp-37A1,* and *ugt-29*) differentially expressed by at least ten percent upon *ahr-1* RNAi (**Figure EV1; Appendix Table S1**). Unexpectedly, when crossed into the *ahr-1(ju145)* mutant background, we observed different effects for *cyp-35B1* and *gst-4* expression, while the expression of *ugt-29* remained reduced in the *ahr-1* mutant

(**Figure EV1 C, D, E**), suggesting either different mode of action of *ahr-1* silencing and mutation or tissue-specific effects disclosed by the RNAi treatment. In line with the differential effect between *ahr-1* RNAi and mutant on *cyp-35B1* and *gst-4* expression, *ahr-1* suppression by RNAi did not have any impact on the lifespan of the wild-type animals (**Table 1; Figure EV1 G**). Moreover, when *ahr-1* RNAi was fed to different *C. elegans* strains, in which silencing is effective only or primarily in specific tissues (Calixto, Chelur et al., 2010, Espelt, Estevez et al., 2005, Kumsta & Hansen, 2012, Qadota, Inoue et al., 2007, Schmitz, Kinge et al., 2007, Sijen, Fleenor et al., 2001, Tijsterman, Okihara et al., 2002, Yigit, Batista et al., 2006), we observed that in most cases tissue-specific *ahr-1* RNAi did neither affect health- or lifespan, which were instead significantly shortened only when RNAi was applied systemically but enhanced in the nervous system (**Table 1; Figure EV1 F**). Taken together these data reveal that a complex AHR-1 role in *C. elegans'* lifespan and response to stress in a tissue- and insult-dependent manner.

AHR-1 differentially regulates lifespan in response to potential modulators of its activity

AhR knockout in basal conditions revealed its role in aging and other physiological processes (Eckers et al., 2016, Mulero-Navarro & Fernandez-Salguero, 2016), yet, in mammals, AhR primarily exerts its functions in response to several different ligands and modulators of its activity, namely exogenous substances such as xenobiotics or dietary compounds, and endogenous products of metabolism such as tryptophan derivatives and microbiota-associated factors (Lee et al., 2017). Thus, we then investigated whether representative AhR modulators of each class affect *C. elegans* life traits and gene expression through AHR-1. The polyphenol curcumin is a dietary component well known to extend lifespan in *C. elegans* and can modulate AhR signaling in mammals (Amakura et al., 2003, Liao, Yu et al., 2011, Nishiumi, Yoshida et al., 2007). Consistent with a potential conserved activity through AhR, curcumin reproducibly and significantly extended life- and health-span in an *ahr-1*-dependent

manner (**Figure 2 A, B; Figure EV2 A**). In human cancer cell lines, curcumin alters the expression of the AhR target genes *Cyp1A1* and *Cyp1B1* (Choi, Chun et al., 2008, Rinaldi, Morse et al., 2002). However, quantification of 47 *C. elegans cyp*s by quantitative PCR revealed that only *cyp-13B1* was significantly upregulated either by *ahr-1* depletion or by curcumin in an *ahr-1*-dependent manner in *C. elegans*, while other two *cyps* (i.e. *cyp-13A5* and *cyp-13A8*) were increased in an *ahr-1*-independent manner (**Figure EV2 B - D**). In mammals, AhR-mediated induction of *cyps* mediates some of the toxic effects of the xenobiotic BaP (Shimizu et al., 2000) and in *C. elegans* BaP induces *cyp* genes expression *(Menzel, Bogaert et al., 2001)*. We observed that although BaP significantly increased the expression of the *cyp-35B1* reporter strain and affected animals' development in a dose-dependent manner, these effects were largely *ahr-1*-independent (**Figure S3 A, B**). Of note, we found that BaP treatment from adulthood, consistent with its toxic effects, significantly shortened animals' health- and lifespan, with a more pronounced effect on *ahr-1* mutants, indicating a protective role of AHR-1 against BaP-curtailed longevity (**Figure 2 C, D**).

As opposed to the exogenous modulators, 6-formylindolo[3,2-b]carbazole (FICZ), a photoproduct of tryptophan produced in response to UVB light, is a well-described AhR endogenous high-affinity ligand (Fritsche et al., 2007, Rannug et al., 1987). In *C. elegans* UVB radiation shortens lifespan, induces embryonic lethality and germline cells apoptosis in a dose-dependent manner (Lans, Marteijn et al., 2010, Torgovnick, Schiavi et al., 2018). In Fig 1 we showed that *ahr-1(ju145)* embryos derived from irradiated meiotic cells - those prompted to undergo apoptosis - are more sensitive to UVB-induced embryonic lethality. In line with these results, we found that UVB-induced germline cells apoptosis was significantly more increased in the *ahr-1* mutant's germline compared to wild-type animals (**Figure S3 C**). UVB irradiation increases *Cyp1A1* expression in human keratinocytes in an AHR-dependent manner (Fritsche et al., 2007). Interestingly, similar to the above results with BaP, although UVB tent to increase *cyp-35B1* expression in an *ahr-1*-independent manner (**Figure S3 D**), it decreased animals' lifespan and motility with a significantly stronger effect on the

ahr-1(ju145) compared to wild-type animals (**Figure 3 E, F**). These results agree with the notion that loss of AhR sensitizes mammalian cells to UVB-induced apoptosis (Frauenstein, Sydlik et al., 2013) and support an evolutionarily conserved role of AhR in response to UVB.

Finally, to assess the possible interaction of AhR with microbiota-associated factors we took advantage of two commonly used *Escherichia coli* strains used as a food source for *C. elegans*, HT115(DE3) and OP50(xu363). We observed that, consistent with the growing body of evidence indicating a crosstalk between microbiota and AhR in mammals, the activation of a *cyp-35B1*-GFP reporter was reduced in the absence of *ahr-1* when animals were fed HT115 but not OP50 (**Figure EV3 F**). Strikingly, we found that the beneficial effects on lifespan, motility, pharyngeal pumping, and heat resistance elicited in the *ahr-1* mutants fed HT115 are completely abolished when animals are fed OP50 (**Figure 3 G, H; Figure EV3 E, G**). These differences are neither due to extrinsic bacterial differences nor to the effect of the two different bacteria on the *ahr-1* expression (**Figure EV3 H**) thus likely relying on the modulation of AHR-1-regulated processes.

Results described so far indicate that known AhR modulators differentially affect *C. elegans* lifespan in an *ahr-1*-dependent manner but that classical detoxification related genes (*cyp*s) are possibly not the major targets of *C. elegans* AHR-1. Thus, to gain insight into molecular mechanisms of AhR-regulated stress response and aging we turned to the results of a transcriptomic analysis recently carried out in the lab, which, according to the described role of *C. elegans* AHR-1 in neuronal determination (Huang et al., 2004, Qin & Powell-Coffman, 2004, Qin et al., 2006, Smith et al., 2013), revealed enrichment in processes linked to neuronal development and differentiation (Brinkmann et al. *in preparation*). A thorough analysis of the most differentially expressed genes between wild-type and *ahr-1(ju145)* revealed that many of them have been described in *C. elegans* to be affected not only during aging but also by dietary compounds (e.g. quercetin, resveratrol, bacteria) known to modulate AhR activity in mammals (**Appendix Tables S2, S3**). Interestingly, quantitative PCR analysis of some of these genes (*atf-2, K04H4.2, egl-46, T20F5.4, ptr-4, dyf-7, clec-*

209, C01B4.6, C01B4.7, F56A4.3) confirmed their *ahr-1* dependency in basal conditions and identified a specific AhR-bacteria diet regulatory effect (**Figure EV4**). Namely, while UVB or curcumin did not influence the expression of these genes neither in wt nor in the absence of the *ahr-1*, the reduced expression of the genes in the *ahr-1(ju145)* mutants fed HT115 was abolished in animal fed and OP50 diet (**Figure EV4**). Altogether, results shown so far support an evolutionarily conserved protective role for AhR against BaP and UVB and identify a new role for AhR in environmentally regulated aging with dietary bacteria as an important component in *ahr-1*-signaling-mediated longevity.

Loss of *ahr-1* affects age-associated pathologies in a diet-dependent manner

The critical role of AHR-1 in *C. elegans* neurons (Huang et al., 2004, Qin & Powell-Coffman, 2004, Smith et al., 2013) and motility (Eckers et al., 2016, Williams et al., 2014) prompted us to investigate whether diet-dependent effects also influence age-related neuromuscular pathologies. A growing body of evidence indeed indicates microbiota can affect various aspects of *C. elegans'* health-span (Brooks, Liang et al., 2009, Maier, Adilov et al., 2010, Munoz-Lobato, Rodriguez-Palero et al., 2014, Reinke, Hu et al., 2010, Xiao, Chun et al., 2015). In line with previous results, loss of *ahr-1* extended life- and health-span of two age-associated disease models, namely animals with muscle expression of aggregation-prone proteins polyQ$_{40}$ (Morley, Brignull et al., 2002) and α-synuclein (van Ham, Thijssen et al., 2008) (**Figure 3**). Strikingly, when we looked at the diet-dependent effects, we found that similar to the wild-type strain, also the life- and health-span improvement promoted by *ahr-1* deficiency in these disease models were significantly suppressed when animals were fed an OP50 diet instead of HT115 (**Figure 3 A, B, E, F**). Somewhat to our surprise, despite being longer-lived, *ahr-1* mutants fed HT115 displayed a greater number and size of polyQ$_{40}$ and α-synuclein aggregates, which is nonetheless in line with studies revealing no direct correlation between aggregates and toxic effects (van der Goot, Zhu et al., 2012). Of note, the increase

in aggregation was mainly regulated in a diet-independent manner (**Figure 3 C, D, G, H**), indicating that the *ahr-1*-diet interaction effect on health-span is independent of its effect on protein aggregation. Very surprisingly, when we investigated the effect of *ahr-1* deficiency in another pro-aggregation model - a *C. elegans* strain expressing a pan-neuronal human $A\beta_{1-42}$ peptide (Fong, Teo et al., 2016) - we found that contrary to the other models, it reduced animals' life- and health-span, yet interestingly in a diet-dependent manner (**Figure EV5**).

Given that temperature may affect aging and associated pathologies depending on the bacterial diet and genetic background (Maier et al., 2010, Miller, Fletcher et al., 2017) we next tested whether the healthy aging phenotype of *ahr-1* is also temperature-dependent. Despite the increased resistance to heat shock of *ahr-1(ju145)* mutants, and opposite to the lifespan at 20 °C, *ahr-1* mutants were short-lived on an HT115 diet at 25 °C. Yet, again, this difference in the lifespan of wild-type and *ahr-1* was abolished on the OP50 diet, which *per se* already shortened the lifespan at 25 °C of wild-type animals (**Figure 4 A, B**). The higher temperature also prevented the beneficial diet-dependent effects of loss of *ahr-1* on life- and health-span in the polyQ strain (**Figure 4 C, D**), while the number of polyQ aggregates increased according to the rise in temperature but still in a diet-independent manner (**Figure 4 E, F**). Overall our data revealed a new diet-dependent, protein aggregation-independent effect of AhR in modulating age-associated neuromuscular pathologies.

Bacterial tryptophan metabolism mediates the beneficial effect of the *ahr-1* mutants

In search of the potential bacterial factor responsible for the diet-dependent effects, we first asked whether metabolically active bacteria are required for the observed differences. To this end, we compared the heat-stress resistance of animals fed alive bacteria with that of animals fed bacteria either killed before seeding on plates or killed on the plates two days after seeding (thus allowing metabolites secretion). Very interestingly, killing bacteria before seeding completely abolished the differences between wild-type and *ahr-1* fed HT115

(**Figure 5 A – B**), indicating that a factor produced by metabolically active HT115 bacteria may influence the AHR-1-mediated effects. In support of this possibility, the increased resistance to stress of *ahr-1* animals observed on living HT115 bacteria persisted when bacteria were killed after growing for two days on the feeding plates (**Figure 5 C**). In line with the heat shock experiments, killing the bacteria before seeding also completely suppressed the increased lifespan of the *ahr-1* mutants on HT115 with no major effects on animals fed OP50 (**Figure 5 D**). These data point towards HT115 secreted metabolites playing a role in *ahr-1*-mediated life- and health-span, likely via gut ingestion or neuronal sensing (Maier et al., 2010). In mammals, tryptophan (Trp) and its metabolites (such as indole) modulate AhR activity (Jin et al., 2014, Manzella, Singhal et al., 2018, Miller, 1997) and in *C. elegans* Trp was shown to abolish some of the different phenotypes observed between alive HT115 and OP50 (Gracida & Eckmann, 2013). Of note, supplementation of L-tryptophan completely abolished the heat-stress resistance of *ahr-1(ju145)* on HT115 - and partially suppressed the difference also between wild-type and *ahr-1(ju145)* on OP50 (**Figure 5 E, F**). Mass spectrometric analysis of the two bacteria supernatants revealed that the subtracted spectrum between HT115 and OP50 showed three prominent peaks (**Figure 5 G**) with m/z 361 likely being an arginine-tryptophan dipeptide, thus supporting a role for Trp in mediating the differential effects observed between HT115 and OP50. Overall, these data point towards a potential role in Trp metabolism in modulating *ahr-1*-bacteria-regulated age-associated phenotypes.

Discussion

C. elegans AHR-1, similar to mammalian AhR, forms a heterodimer with the *C. elegans* Arnt homolog AHA-1 and binds to xenobiotic responsive elements (XREs), but unlike its mammalian counterpart, it does not bind the classical AhR activators such as TCDD or β-naphthoflavone (Powell-Coffman et al., 1998). However, no other potential AhR ligands or ligand-independent modulators have ever been tested in *C. elegans*, thus precluding to fully exploit the versatility of this model organism to unravel conserved or novel biological function for this environmentally relevant transcription factor. Only recently, conserved functions of the *C. elegans* AHR-1 in health and lifespan (Eckers et al., 2016, Williams et al., 2014) have been identified.

In this new study, we revealed a more general and complex role for this transcription factor in stress response and aging in basal conditions and in response to known modulators of its activity (i.e. curcumin, UVB and BaP). The differential effects on lifespan and gene expression we observed upon *ahr-1* genetic- or RNAi-mediated suppression interestingly reveal the importance of fine-tuning its activity in a dose and/or tissue-dependent manner, which very nicely recapitulate the variety of phenotypic features described in mammals upon dosage effects or tissue-specific depletion (Brinkmann et al., 2020). Moreover, to our surprise, we found that besides increased resistance to heat-shock, lack of *ahr-1* did not confer resistance to any other investigated insult, such as metabolic stress or radiation, and in fact sensitize animals to UVB. We specifically decided to focus our attention on the influence on stress response and aging of different classes of mammalian AhR modulators: environmental (xenobiotic) and dietary factors as well as by microbiota and endogenous factors produced by the organism. These mainly induce AhR's transcriptional activity in a ligand-dependent manner, but ligand-independent, as well as antagonistic functions, have been also suggested (Ashida et al., 2008). Our data showed that *C. elegans ahr-1(ju145)* mutants are more sensitive to the lifespan shortening effects of UVB and BaP, two classical

activators of mammalian AhR, thus further supporting a role for *ahr-1* in the aging process. Of note, *ahr-1* mutants also conferred sensitivity to UVB-reduced fertility, which we hypothesized to reflect increased sensitivity to germ cells apoptosis in irradiated animals as also found in human keratinocytes and mice (Frauenstein et al., 2013, Pollet, Shaik et al., 2018). Indeed, loss of AHR-1 function increased apoptosis in basal condition and upon radiation indicating a conserved anti-apoptotic function of the AhR in response to UVB. Similar to the detrimental effect of UVB, exposure to BaP in mammals decreases the lifespan and causes a variety of cancers as well as neurotoxicity (Chepelev, Moffat et al., 2015, Sakakibara, Nakagawa et al., 2005), and loss of AhR prevents BaP- and UVB-induced carcinogenicity in mice (Pollet et al., 2018, Shimizu et al., 2000). In this study, we showed for the first time that BaP has a conserved detrimental effect on lifespan, which is significantly worsened in the *C. elegans ahr-1* mutants. Along with the UVB data, these findings support a protective role of AHR-1 in response to classical mammalian activators. However, surprisingly, both stressors induced *cyp-35B1* expression in an *ahr-1*-independent manner thus pointing to a non-canonical mode of activation of AHR-1 in *C. elegans*. Interestingly, BaP and the UVB-generated ligand FICZ are big and planar molecules which, based on preliminary *in silico* analysis (Brinkmann et al. *in preparation*) likely do not fit into the ligand binding pocket of the *C. elegans* AHR-1. Thus, one can speculate that AHR-1, like its mammalian homolog, is activated by reactive oxygen species (ROS) (Kubli, Bassi et al., 2019), which can be produced either by UVB (Heck, Vetrano et al., 2003) or BaP (Cui, Chen et al., 2019, Wu, Huang et al., 2015).

Modulation of AHR-1 activity by ROS could also explain the potential inhibitory effect of curcumin on AHR-1. Indeed, polyphenols are dietary AhR modulators (Xue et al., 2017) with conserved beneficial effects on health and aging from invertebrates to humans (Monroy, Lithgow et al., 2013) often ascribed to their antioxidant properties (Liao et al., 2011). Here we found that curcumin promotes life- and health-span depending on *ahr-1* but, similar to the other modulators, it did not modulate the expression of classical *ahr-1*-dependent genes

such as *cyps*. Interestingly, curcumin and AHR-1 loss-of-function lead to non-additive effects on lifespan extension compared to untreated wild-type animals, suggesting that curcumin might actually act as an AHR-1 inhibitor, as also reported in mammals (Nishiumi et al., 2007). Whether the effects of curcumin are mediated through direct binding to AHR-1 or indirect modulation of its activity through other mechanisms (e.g. ROS reduction) remain to be clarified but our preliminary *in silico* analysis suggests that it is unlikely through a direct binding of curcumin to the AHR-1 ligand binding domain. Accordingly, while direct ligand-binding has not been verified for many of the polyphenolic AhR modulators, ligand-independent effects on AhR signaling, like binding to HSP90 (Palermo, Westlake et al., 2005) or inhibition of AhR phosphorylation by the protein kinase C (Das, Ramani et al., 2016, Nishiumi et al., 2007) , have been instead described.

Most notably, we identified for the first time a critical role for AHR-1-bacterial diet interaction in regulating aging and associated phenotypes. Specifically, *ahr-1* mutants displayed an extended health- and life-span on HT115 but not on the OP50 bacterial diet. Loss of *ahr-1* also ameliorated health- and life-span in models of age-associated pathologies with aggregation-prone proteins expressed in the muscles in a diet-dependent manner. Yet, surprisingly, the beneficial effect did not correlate with the amount and size of the aggregates, indicating either that aggregation in this context actually has a beneficial effect, or that loss of *ahr-1* promotes health-span independently from mechanisms regulating proteotoxic aggregation. Regardless, we hypothesized that bacteria-associated factors from HT115 or OP50 might mediate the diet-dependent changes in health-span and narrowed them down to secreted bacterial metabolites. Although the exact metabolite(s) responsible for the diet-dependent effects still remain to be identified, our data point to the potential involvement of Trp metabolism. This again supports evolutionarily conserved functions of AHR-1, as its activity is known to be influenced by Trp and its metabolites in mammals (Jin et al., 2014, Manzella et al., 2018, Miller, 1997). Interestingly, Trp and its metabolites have been already shown to differentially modulate *C. elegans'* health- and life-span. Trp

supplementation increases heat-stress resistance and lifespan of *C. elegans* (Edwards, Canfield et al., 2015) and reduces the proteotoxicity in neurodegenerative disease models (van der Goot et al., 2012). Instead, different Trp metabolites display opposite effects: Trp degradation through the Kynurenine pathway increases proteotoxicity in neurodegenerative disease models (van der Goot et al., 2012), while the tryptophan metabolite indole, from commensal bacteria, increases the lifespan of *C. elegans* through AHR-1 (Sonowal, Swimm et al., 2017). The primary site of action of the bacterial metabolite (e.g. intestine, sensory neurons) as well as the affected AhR-dependent molecular process involved in modulation of the aging process (e.g. immune response, redox reactions), are very challenging and interesting points which remain to be addressed.

In summary, we demonstrated that *C. elegans ahr-1* displays evolutionarily conserved functions, such as its protective activity against xenobiotic and UVB, but opposite roles in the aging process in response to environmental or dietary interventions. Most importantly, we identified a direct link between *ahr-1*-regulated processes and bacterial diet as a key determinant of aging and associated pathologies, most likely trough tryptophan metabolism. Overall our findings support a central role for AhR in the aging process in a context-dependent manner, thus expanding the already vast panel of activities played by the AhR in different pathophysiological conditions and establishing *C. elegans* as a powerful model organism to unravel new AhR-regulated processes in response to conserved modulators of its activity.

Material and Methods

C. elegans strains and cultivation

C. elegans strains used in this study are listed in **Appendix Table S4**. We created the following strains for this study by crossing CZ2485 with different transgenic strains to obtain: NV33a: *ahr-1(ju145); cyp-35B1p::GFP* + *gcy-7p::GFP*, NV35a: *ahr-1(ju145); (pAF15)gst-4p::GFP::NLS*, NV38b: *ahr-1(ju145); unc-54p::Q40::YFP*, NV42a: *ahr-1(ju145); unc-54p::alpha-synuclein::YFP,* NV43a: *ahr-1(ju145)*; *hsp-6p::GFP,* NV47a: *ahr-1(ju145*); *ugt-29*p::GFP. For maintenance, worms were kept synchronized by egg lay at 20 °C on Nematode Growth Media (NGM) plates and fed with *E. coli* OP50 according to methods described in (Stiernagle, 2006). For the experiments, worms were synchronized on plates supplemented with *E. coli* HT115(L4440) or OP50(L4440) according to the condition of interest. Unless stated otherwise, plates were supplemented with 1 mM IPTG when using HT115(L4440) or OP50(L4440).

Crossing CZ2485 with transgenic strains

CZ2485 males were generated by treating hermaphrodite L4 larvae with heat stress (4 h at 30 °C). 10 adult CZ2485 males were then left with one hermaphrodite L3/L4 larvae for mating (P0 generation). Single worms of the F1 and F2 generations of this cross were checked for the *ju145* allele by PCR (ahr-1F `CGGAAAGTTGATGTCTCTAC`, ahr-1R `TGCTGACTAGACGATATACC`) followed by a restriction with *AlwI* (New England Biolabs, R0513S), which cuts the PCR fragment at the position of the *ju145* point mutation. Single worm PCR was performed according to standard protocols (He, 2011).

Gene silencing by RNA-mediated interference (RNAi)

Gene silencing was achieved through feeding bacteria expressing plasmids with dsRNA against specific genes (Timmons & Fire, 1998). For RNAi, either *E. coli* HT115(DE3) or *E. coli* OP50*(xu363)* (Xiao et al., 2015) were used. RNAi feeding was applied continuously from birth to death.

E. coli strains and growth

Bacteria were grown in LB medium at 37 °C overnight. When using *E. coli* carrying vectors the LB medium was supplemented with 0.01 % of ampicillin and 0.0005 % of tetracycline. *E. coli* HT115(L4440), HT115(*ahr-1*), and OP50 were obtained from the Ahringer *C. elegans* RNAi library (Kamath & Ahringer, 2003). *E. coli* OP50*(xu363)* was a gift from Shawn Xu.

Transformation of *E. coli* OP50(xu363)

For this study, we created OP50(L4440) by PEG transformation of OP50(xu363) according to methods described previously with adjustments (Chung & Miller, 1988). 100 µl of OP50(xu363) were transformed with 100 pg of plasmids isolated from the HT115(DE3) strains (Ahringer Library). The QIAprep Spin Miniprep Kit (Qiagen, 27104) was used for plasmid isolation.

Heat stress survival

The resistance to heat stress was tested with 20 animals/condition per experiment at 35 °C on 3 cm plates wrapped with parafilm in an incubator (Intrafors HT Multitron). When using animals older than 3 days, animals were transferred to fresh NGM plates daily during the fertile phase. The number of dead animals was scored hourly by gently touching the worms with a platinum wire and analysis was performed as described for the lifespan assay.

Reproduction on heat stress, glucose, and BP

Animals were grown on control plates with alive bacteria until day 3 and then transferred to treatment or control plates for 24 hours. After a 24-hour treatment, 3 animals of each condition were transferred to fresh control plates for 4 hours to lay eggs and the number of eggs laid was counted. The number of progenies hatched from these eggs was counted 2 days afterward.

Development

The development on the specific compound was explored by counting the number of eggs, which developed to gravid adults after 72, 96, and 120 hours as well as the number of worms that arrested their development and the number of eggs, which did not hatch.

Glucose treatment

D-Glucose (Merck, 8342) was dissolved in H_2O and supplemented to the NGM after autoclaving and UVB killed *E. coli* HT115(L4440) were fed as a food source.

2,2′-dipyridyl (BP) treatment

The iron chelator 2,2′-dipyridyl (Carl Roth, 4153) was dissolved in H_2O and supplemented to the NGM after autoclaving.

UVB irradiation

Worms were exposed to ultraviolet radiation on bacteria-free NGM plates, using a Waldmann UV 236 B (UV6) lamp with an emission maximum of 320 nm. Irradiation times were 9 seconds, 27 seconds, and 53 seconds for 100 J/m², 300 J/m² and 600 J/m², respectively with a distance of 18 cm between lamp and plate.

Reproduction after UVB treatment

3 days old worms were treated with UVB and the effect of irradiation on germ-cells in different stages (oogenic stage, meiotic stage, and mitotic stage) was investigated, as described in (Kim, Yang et al., 2005). Briefly, the number and viability of eggs laid between 1 – 8 hours (oogenic stage), 8 – 24 hours (meiotic stage) and 24 – 32 hours (mitotic stage) after the irradiation were analyzed.

Lifespan

The lifespan analysis was started from a synchronized population of worms, which was transferred to fresh NGM plates daily during the fertile period. After the fertile phase, the animals were transferred every alternate day. Dead, alive and censored animals were scored during the transferring process. Animals were counted as dead when they did show neither movement, nor response to a manual stimulus with a platinum wire, nor pharyngeal pumping

activity. Animals with internal hatching (bags), an exploded vulva or which died desiccated on the wall were censored. The number of dead and censored animals was used for survival analysis in OASIS (Yang, Nam et al., 2011) or OASIS 2 (Han, Lee et al., 2016). For the calculation of the mean lifespan and the survival curve in OASIS and OASIS 2, the Kaplan Meier estimator was used, and the p-values were calculated using the log-rank test between pooled populations of animals.

Movement/Healthspan

The movement was set as a parameter for healthy aging, and the phase of active movement is referred to as healthspan. It was assessed in the populations used for the lifespan assay. Animals, which were either crawling spontaneously or after a manual stimulus, were considered as moving while dead animals or animals without crawling behavior were considered as not moving. Statistical analysis was done as described for lifespan.

Curcumin treatment

Curcumin (Sigma Aldrich, C7727) was dissolved in DMSO (Carl Roth, 4720) in a concentration of 100 mM and supplied to the NGM after autoclaving. The final concentration of curcumin in the media was 100 µM (0.1 % DMSO). Control plates contained 0.1 % DMSO. Worms were treated continuously starting from eggs.

Benzo(a)pyrene (BaP) treatment

Benzo(a)pyrene (Sigma Aldrich, B1760) was dissolved in DMSO (Carl Roth, 4720) in concentrations 1000 times higher than the desired concentration in the NGM. After autoclaving the NGM, BaP or DMSO were added to the media. For development assays, worms were treated from eggs, while they were treated from the first day of adulthood for lifespan and healthspan assays.

Quantification of polyQ aggregates

PolyQ$_{40}$ aggregates were visualized by fluorescence microscopy (100x magnification) in worms anesthetized with 15 mM sodium azide (Sigma, S2002). The number and the size of

the aggregates were quantified in Fiji (Schindelin, Arganda-Carreras et al., 2012). To assess the number of aggregates, images were stitched using the Fiji pairwise stitching plugin (Preibisch, Saalfeld et al., 2009) to create whole worms. The average size of the aggregates was instead measured in the non-stitched images. The number and the size of aggregates were counted using the plugin “Analyze Particles”.

Quantification of α-synuclein aggregates

α-synuclein aggregates in the head muscles of 7-days old worms were visualized by fluorescence microscopy (400x magnification) in worms anesthetized with 15 mM sodium azide (Sigma, S2002). Pictures were segmented using Ilastik (version 1.3.0) (available on https://www.ilastik.org/) (Sommer, Strähle et al., 2011). The segmented pictures were used to analyze the number and size of the aggregates in Fiji (Schindelin et al., 2012) using the plugin “Analyze Particles”.

Assessment of age-associated features at 25 °C

Lifespan, movement, and polyQ aggregation analysis were performed as described above. PolyQ-expressing worms were kept at 20 °C until reaching the L4 stage and were afterward kept at 25 °C for the rest of their lifespan.

Killing bacteria before seeding

When seeding killed *E. coli* onto the NGM, the bacteria were pelleted (10 min at 4000 rpm), the supernatant was removed, and the pellet was suspended in S-basal to a final concentration of OD_{595} = 3.6. Then the bacteria suspension was irradiated with a UVB lamp (Waldmann UV 236 B) for 1 hour to kill the bacteria. The suspension of the dead bacteria was again pelleted and re-suspended in fresh S-basal. Killed bacteria were seeded to NGM plates in a concentration of OD_{595} = 3.6 and let dry at room temperature overnight.

Killing bacteria on plates

Bacteria (OD_{595} = 0.9) were seeded to the NGM plates and let grow for 2 days at room temperature. The bacterial lawn was then killed by exposure to UVB light (Waldmann UV 236 B) for 45 min.

Tryptophan supplementation

The concentration of tryptophan and the supplementation procedure was taken from (Gracida & Eckmann, 2013) with minor changes. L-tryptophan (Carl Roth 4858.2) was dissolved in water at a concentration of 12.5 mg/ml and incubated shaking at 30°C for 45 min. Afterward, the solution was filtered (pore size: 0.22 µm, Carl Roth P666.1). For 7 ml of NGM 200 µl of 12.5 mg/ml tryptophan was spotted on the bacterial lawn of an NGM plate, which was kept at room temperature for overnight. After the supplementation, the dish was kept at room temperature for another day.

Mass Spectrometry

Liquid NGM was prepared like solid NGM but without agar to prevent solidification. NGM was poured into petri dishes (7 ml NGM/ 6 cm petri dish) and seeded with bacteria (200 µl, OD_{595} = 0.9) or LB-medium (control). The medium was incubated for two days at room temperature to allow the bacteria to grow. Then, the bacteria were removed by centrifugation (4500 rpm, 10 min) and the medium was filtered (22 µm filter, Carl Roth P666.1) before using it for mass spectrometry analysis. Electrospray ionization mass spectrometry (ESI-MS) was used. For the LC-MS measurements, the liquid NGM samples were diluted 1:20 with methanol before the injection of 10 µl sample volumes. Triterpenes were separated on a Dionex HPG 3200 HPLC system (Thermo Scientific) equipped with a 150 x 2.1 mm, 2.7 µm, C18-CSH column (Waters) with a binary gradient system. Mobile phase A consisted of water + 0.1 % formic acid (FA), and mobile phase B consisted of methanol + 0.1 % FA. The mobile phase gradient was as follows: Starting conditions were 5 % mobile phase B, increased to 95 % B within 10 min, the plateau was held for 4 min, and the system was returned to starting conditions within 1 min and held for another 4.5 min. The flow rate was 0.5 mL/min. The MS and MS/MS analysis were performed with a quadrupole-time-of-flight instrument (maXis 4G, Bruker

Daltonics, Bremen, Germany) equipped with an ESI source. The device was operated in positive-ion and negative-ion mode and the operating conditions were as follows: dry gas (nitrogen): 8.0 L/min, dry heater: 220 °C, nebulizer pressure: 1.8 bar, capillary voltage: 4500 V. Data analysis were performed using the software data analysis 4.2 and Metabolite detect 2.1 (Bruker daltonics, Bremen, Germany).

Quantification of transgene expression

The expression of fluorescently-tagged genes was investigated in adult worms (first day of adulthood) by using fluorescence microscopy (ZEISS Imager M2 with an Axiocam MRm camera). For this, worms expressing fluorescently tagged genes were paralyzed with 15 mM NaN_3 and pictures were taken with identical exposure times and settings. The pictures were then analyzed in either Image J, Fiji (Schindelin et al., 2012) or cellprofiler. Depending on the distribution of the expression, the fluorescence was either measured in a defined area of the region of interest or the whole worm. Statistical analysis was performed with the pooled data.

Measurement of *cyp-35B1p::GFP* intensity in response to BaP

3-days old worms were treated with BaP or UVB for 18 hours. The relative intensity of *cyp-35B1p::GFP* was then visualized by fluorescence microscopy (100x magnification) and analyzed using Fiji (Schindelin et al., 2012). The integrated density was chosen as a parameter for the expression. The quantified intensities were normalized to the mean of untreated wild-type in each experiment. Statistical analysis was performed with the pooled data.

UVB-induced Apoptosis

To investigate UVB-induced apoptosis, L4 larvae were treated with 600 J/m² UVB and the apoptotic corpses were counted 24 h post-irradiation in the gonad loop region. The apoptotic corpses were identified based on their shape.

Fertility

The number of eggs and progeny of animals were investigated during the main fertile period. Two days after synchronization single L4 larvae were transferred to NGM plates and from then transferred to fresh NGM plates every 24 hours until the 8th day after hatching. The number of eggs laid during this period was counted. Two days later the progeny hatched on each day were counted.

Pharyngeal pumping using the NemaMetrix ScreenChip System

To measure the pharyngeal pumping rate with the NemaMetrix ScreenChip, worms were washed off the plates with S-basal and collected in a reaction tube. Then, the worms were washed twice with S-basal and twice with 10 mM serotonin (Sigma Aldrich, 14927) and incubated in 10 mM serotonin for 30 min. Worms were loaded on the ScreenChip SC40 with a syringe (0.01 ml – 1 ml). The EPG of single worms was recorded for a duration of approx. 2 minutes. Only worms which showed pumping activity were recorded, while those with no pumping activity were not considered. The following NemAcquire-2.1 and NemAnalysis-0.2 software were used for analysis (https://nemametrix.com/products/software/).

Assessment of mRNA expression by RTqPCR

Samples from 3 independent replicates with approximately 1000 3-days old worms per condition were collected and RNA was extracted. After washing and elution steps the RNA content was quantified by spectrophotometry, and 1 - 2 µg of RNA was used for the cDNA synthesis (Omniscript RT Kit (Qiagen, 205111). Primers were designed using NCBI Primer BLAST (https://www.ncbi.nlm.nih.gov/tools/primer-blast/) (Ye, Coulouris et al., 2012). Each primer pair was designed to span an exon-exon junction. Primer pairs and their features are listed in **Appendix Tables S5 – S6**. For the Real-time qPCR, the cDNA was diluted 1:20 in 10 mM TRIS (pH 8.0). For the reaction, the qPCR Green Core kit (Jena Biosciences, PCR-333L) or the GoTaq® qPCR kit (Promega, A6001) was used. The samples were run in a MyiQ2 cycler (BioRad), and the expression of each sample was measured in duplicate on the same multi-well plate. The expression was calculated relative to the reference genes *act-1* and *cdc-42* using the iQ5 software. All data collected were enabled for gene study

according to the BioRad user instructions, and the expression was calculated using the normalized expression (ddC_T). The efficiency of each primer pair reaction was added for correct quantification of the normalized expression. The efficiency was assessed with 1:20, 1:100, 1:500, and 1:2500 dilutions of the cDNA. From normalized expression values, the fold-change compared to wild-type was calculated for each replicate.

Statistical analysis

If not stated, statistical analysis was performed in GraphPad Prism 6. For life-/healthspan assays, statistical analysis was done using OASIS (Han et al., 2016, Yang et al., 2011). Statistical analysis of the microarray data was performed in R.

Acknowledgments

Most nematode strains utilized in this work were provided by the Caenorhabditis Genetics Center, funded by the NIH Office of Research Infrastructure Programs (P40 OD010440). Other nematodes or bacteria strains were kindly provided by David Depomerai (University of Nottingham), Sheila Nathan (University of Malaysia), and Shawn Xu (University of Michigan). We thank Anne Hemmers, Bo Scherer, and Lisa Tschage for technical help, Sabine Metzger (University of Cologne) for the performance of mass spectrometry, and Rene Deenen (University of Düsseldorf) for the performance of the microarray. We further thank Wormbase and the GENiE network funded by the European Cooperation in Science and Technology (COST Action BM1408). This work was financially supported by funding to N.V. from the German Research Foundation (DFG VE366/8-1). V.B. was supported by a Ph.D. scholarship by the Jürgen Manchot Foundation.

Author Contributions

Conceptualization: N.V.

Formal analysis: V.B., A.Sc., N.V.

Funding acquisition: V.B., N.V.

Investigation: V.B., D.P., A.Sh.

Supervision: N.V.

Resources: R.M., N.V.

Visualization: V.B.

Writing -original draft-: V.B., N.V.

Writing -review and editing-: R.M., A.Sc.

Conflict of interest

The authors declare no competing interests.

References

Aarnio V, Storvik M, Lehtonen M, Asikainen S, Reisner K, Callaway J, Rudgalvyte M, Lakso M, Wong G (2010) Fatty acid composition and gene expression profiles are altered in aryl hydrocarbon receptor-1 mutant Caenorhabditis elegans. *Comp Biochem Physiol C Toxicol Pharmacol* 151: 318-24

Alavez S, Vantipalli MC, Zucker DJ, Klang IM, Lithgow GJ (2011) Amyloid-binding compounds maintain protein homeostasis during ageing and extend lifespan. *Nature* 472: 226-9

Amakura Y, Tsutsumi T, Sasaki K, Yoshida T, Maitani T (2003) Screening of the inhibitory effect of vegetable constituents on the aryl hydrocarbon receptor-mediated activity induced by 2,3,7,8-tetrachlorodibenzo-p-dioxin. *Biological & pharmaceutical bulletin* 26: 1754-60

Ashida H, Nishiumi S, Fukuda I (2008) An update on the dietary ligands of the AhR. *Expert Opin Drug Metab Toxicol* 4: 1429-47

Brinkmann V, Ale-Agha N, Haendeler J, Ventura N (2020) The Aryl Hydrocarbon Receptor (AhR) in the Aging Process: Another Puzzling Role for This Highly Conserved Transcription Factor. *Frontiers in Physiology* 10

Brooks KK, Liang B, Watts JL (2009) The influence of bacterial diet on fat storage in C. elegans. *PloS one* 4: e7545

Caesar I, Jonson M, Nilsson KP, Thor S, Hammarstrom P (2012) Curcumin promotes A-beta fibrillation and reduces neurotoxicity in transgenic Drosophila. *PloS one* 7: e31424

Calixto A, Chelur D, Topalidou I, Chen X, Chalfie M (2010) Enhanced neuronal RNAi in C. elegans using SID-1. *Nature methods* 7: 554-9

Chepelev NL, Moffat ID, Bowers WJ, Yauk CL (2015) Neurotoxicity may be an overlooked consequence of benzo[a]pyrene exposure that is relevant to human health risk assessment. *Mutation research Reviews in mutation research* 764: 64-89

Choi H, Chun YS, Shin YJ, Ye SK, Kim MS, Park JW (2008) Curcumin attenuates cytochrome P450 induction in response to 2,3,7,8-tetrachlorodibenzo-p-dioxin by ROS-dependently degrading AhR and ARNT. *Cancer science* 99: 2518-24

Chung CT, Miller RH (1988) A rapid and convenient method for the preparation and storage of competent bacterial cells. *Nucleic acids research* 16: 3580

Cui Q, Chen FY, Chen HY, Peng H, Wang KJ (2019) Benzo[a]pyrene (BaP) exposure generates persistent reactive oxygen species (ROS) to inhibit the NF-kappaB pathway in medaka (Oryzias melastigma). *Environ Pollut* 251: 502-509

Cypser JR, Johnson TE (2002) Multiple stressors in Caenorhabditis elegans induce stress hormesis and extended longevity. *J Gerontol A Biol Sci Med Sci* 57: B109-14

Das J, Ramani R, Suraju MO (2016) Polyphenol compounds and PKC signaling. *Biochim Biophys Acta* 1860: 2107-21

Dato S, Rose G, Crocco P, Monti D, Garagnani P, Franceschi C, Passarino G (2017) The genetics of human longevity: an intricacy of genes, environment, culture and microbiome. *Mech Ageing Dev* 165: 147-155

Eckers A, Jakob S, Heiss C, Haarmann-Stemmann T, Goy C, Brinkmann V, Cortese-Krott MM, Sansone R, Esser C, Ale-Agha N, Altschmied J, Ventura N, Haendeler J (2016) The aryl hydrocarbon receptor promotes aging phenotypes across species. *Scientific reports* 6: 19618

Edwards C, Canfield J, Copes N, Brito A, Rehan M, Lipps D, Brunquell J, Westerheide SD, Bradshaw PC (2015) Mechanisms of amino acid-mediated lifespan extension in Caenorhabditis elegans. *BMC Genet* 16: 8

Espelt MV, Estevez AY, Yin X, Strange K (2005) Oscillatory Ca2+ signaling in the isolated Caenorhabditis elegans intestine: role of the inositol-1,4,5-trisphosphate receptor and phospholipases C beta and gamma. *The Journal of general physiology* 126: 379-92

Esser C, Lawrence BP, Sherr DH, Perdew GH, Puga A, Barouki R, Coumoul X (2018) Old Receptor, New Tricks-The Ever-Expanding Universe of Aryl Hydrocarbon Receptor Functions. Report from the 4th AHR Meeting, 29(-)31 August 2018 in Paris, France. *Int J Mol Sci* 19
Fong S, Teo E, Ng LF, Chen CB, Lakshmanan LN, Tsoi SY, Moore PK, Inoue T, Halliwell B, Gruber J (2016) Energy crisis precedes global metabolic failure in a novel Caenorhabditis elegans Alzheimer Disease model. *Scientific reports* 6: 33781
Frauenstein K, Sydlik U, Tigges J, Majora M, Wiek C, Hanenberg H, Abel J, Esser C, Fritsche E, Krutmann J, Haarmann-Stemmann T (2013) Evidence for a novel anti-apoptotic pathway in human keratinocytes involving the aryl hydrocarbon receptor, E2F1, and checkpoint kinase 1. *Cell death and differentiation* 20: 1425-34
Fritsche E, Schafer C, Calles C, Bernsmann T, Bernshausen T, Wurm M, Hubenthal U, Cline JE, Hajimiragha H, Schroeder P, Klotz LO, Rannug A, Furst P, Hanenberg H, Abel J, Krutmann J (2007) Lightening up the UV response by identification of the arylhydrocarbon receptor as a cytoplasmatic target for ultraviolet B radiation. *Proceedings of the National Academy of Sciences of the United States of America* 104: 8851-6
Gracida X, Eckmann CR (2013) Fertility and germline stem cell maintenance under different diets requires nhr-114/HNF4 in C. elegans. *Current biology : CB* 23: 607-13
Han SK, Lee D, Lee H, Kim D, Son HG, Yang JS, Lee SV, Kim S (2016) OASIS 2: online application for survival analysis 2 with features for the analysis of maximal lifespan and healthspan in aging research. *Oncotarget* 7: 56147-56152
He F (2011) Single Worm PCR. *Bio-protocol* Bio101: e60
Heck DE, Vetrano AM, Mariano TM, Laskin JD (2003) UVB light stimulates production of reactive oxygen species: unexpected role for catalase. *J Biol Chem* 278: 22432-6
Huang X, Powell-Coffman JA, Jin Y (2004) The AHR-1 aryl hydrocarbon receptor and its co-factor the AHA-1 aryl hydrocarbon receptor nuclear translocator specify GABAergic neuron cell fate in C. elegans. *Development (Cambridge, England)* 131: 819-28
Ikuta T, Eguchi H, Tachibana T, Yoneda Y, Kawajiri K (1998) Nuclear localization and export signals of the human aryl hydrocarbon receptor. *J Biol Chem* 273: 2895-904
Jin UH, Lee SO, Sridharan G, Lee K, Davidson LA, Jayaraman A, Chapkin RS, Alaniz R, Safe S (2014) Microbiome-derived tryptophan metabolites and their aryl hydrocarbon receptor-dependent agonist and antagonist activities. *Mol Pharmacol* 85: 777-88
Kaeberlein M (2016) The Biology of Aging: Citizen Scientists and Their Pets as a Bridge Between Research on Model Organisms and Human Subjects. *Vet Pathol* 53: 291-8
Kamath RS, Ahringer J (2003) Genome-wide RNAi screening in Caenorhabditis elegans. *Methods (San Diego, Calif)* 30: 313-21
Kim YM, Yang I, Lee J, Koo HS (2005) Deficiency of Bloom's syndrome protein causes hypersensitivity of C. elegans to ionizing radiation but not to UV radiation, and induces p53-dependent physiological apoptosis. *Mol Cells* 20: 228-34
Kubli SP, Bassi C, Roux C, Wakeham A, Gobl C, Zhou W, Jafari SM, Snow B, Jones L, Palomero L, Thu KL, Cassetta L, Soong D, Berger T, Ramachandran P, Baniasadi SP, Duncan G, Lindzen M, Yarden Y, Herranz C et al. (2019) AhR controls redox homeostasis and shapes the tumor microenvironment in BRCA1-associated breast cancer. *Proceedings of the National Academy of Sciences of the United States of America* 116: 3604-3613
Kumsta C, Hansen M (2012) C. elegans rrf-1 mutations maintain RNAi efficiency in the soma in addition to the germline. *PloS one* 7: e35428
Lans H, Marteijn JA, Schumacher B, Hoeijmakers JH, Jansen G, Vermeulen W (2010) Involvement of global genome repair, transcription coupled repair, and chromatin remodeling in UV DNA damage response changes during development. *PLoS genetics* 6: e1000941
Lee HU, McPherson ZE, Tan B, Korecka A, Pettersson S (2017) Host-microbiome interactions: the aryl hydrocarbon receptor and the central nervous system. *Journal of molecular medicine* 95: 29-39

Liao VH, Yu CW, Chu YJ, Li WH, Hsieh YC, Wang TT (2011) Curcumin-mediated lifespan extension in Caenorhabditis elegans. *Mech Ageing Dev* 132: 480-7
Lim GP, Chu T, Yang F, Beech W, Frautschy SA, Cole GM (2001) The curry spice curcumin reduces oxidative damage and amyloid pathology in an Alzheimer transgenic mouse. *J Neurosci* 21: 8370-7
Lopez-Otin C, Blasco MA, Partridge L, Serrano M, Kroemer G (2013) The hallmarks of aging. *Cell* 153: 1194-217
Maier W, Adilov B, Regenass M, Alcedo J (2010) A neuromedin U receptor acts with the sensory system to modulate food type-dependent effects on C. elegans lifespan. *PLoS biology* 8: e1000376
Manzella C, Singhal M, Alrefai WA, Saksena S, Dudeja PK, Gill RK (2018) Serotonin is an endogenous regulator of intestinal CYP1A1 via AhR. *Scientific reports* 8: 6103
Menzel R, Bogaert T, Achazi R (2001) A systematic gene expression screen of Caenorhabditis elegans cytochrome P450 genes reveals CYP35 as strongly xenobiotic inducible. *Arch Biochem Biophys* 395: 158-68
Miller CA, 3rd (1997) Expression of the human aryl hydrocarbon receptor complex in yeast. Activation of transcription by indole compounds. *J Biol Chem* 272: 32824-9
Miller H, Fletcher M, Primitivo M, Leonard A, Sutphin GL, Rintala N, Kaeberlein M, Leiser SF (2017) Genetic interaction with temperature is an important determinant of nematode longevity. *Aging cell* 16: 1425-1429
Monroy A, Lithgow GJ, Alavez S (2013) Curcumin and neurodegenerative diseases. *BioFactors* 39: 122-32
Morley JF, Brignull HR, Weyers JJ, Morimoto RI (2002) The threshold for polyglutamine-expansion protein aggregation and cellular toxicity is dynamic and influenced by aging in Caenorhabditis elegans. *Proceedings of the National Academy of Sciences of the United States of America* 99: 10417-22
Mulero-Navarro S, Fernandez-Salguero PM (2016) New Trends in Aryl Hydrocarbon Receptor Biology. *Front Cell Dev Biol* 4: 45
Munoz-Lobato F, Rodriguez-Palero MJ, Naranjo-Galindo FJ, Shephard F, Gaffney CJ, Szewczyk NJ, Hamamichi S, Caldwell KA, Caldwell GA, Link CD, Miranda-Vizuete A (2014) Protective role of DNJ-27/ ERdj5 in Caenorhabditis elegans models of human neurodegenerative diseases. *Antioxidants & redox signaling* 20: 217-35
Nishiumi S, Yoshida K, Ashida H (2007) Curcumin suppresses the transformation of an aryl hydrocarbon receptor through its phosphorylation. *Arch Biochem Biophys* 466: 267-73
Opitz CA, Litzenburger UM, Sahm F, Ott M, Tritschler I, Trump S, Schumacher T, Jestaedt L, Schrenk D, Weller M, Jugold M, Guillemin GJ, Miller CL, Lutz C, Radlwimmer B, Lehmann I, von Deimling A, Wick W, Platten M (2011) An endogenous tumour-promoting ligand of the human aryl hydrocarbon receptor. *Nature* 478: 197-203
Palermo CM, Westlake CA, Gasiewicz TA (2005) Epigallocatechin gallate inhibits aryl hydrocarbon receptor gene transcription through an indirect mechanism involving binding to a 90 kDa heat shock protein. *Biochemistry* 44: 5041-52
Poland A, Glover E, Kende AS (1976) Stereospecific, high affinity binding of 2,3,7,8-tetrachlorodibenzo-p-dioxin by hepatic cytosol. Evidence that the binding species is receptor for induction of aryl hydrocarbon hydroxylase. *J Biol Chem* 251: 4936-46
Pollet M, Shaik S, Mescher M, Frauenstein K, Tigges J, Braun SA, Sondenheimer K, Kaveh M, Bruhs A, Meller S, Homey B, Schwarz A, Esser C, Douki T, Vogel CFA, Krutmann J, Haarmann-Stemmann T (2018) The AHR represses nucleotide excision repair and apoptosis and contributes to UV-induced skin carcinogenesis. *Cell death and differentiation* 25: 1823-1836
Powell-Coffman JA, Bradfield CA, Wood WB (1998) Caenorhabditis elegans orthologs of the aryl hydrocarbon receptor and its heterodimerization partner the aryl hydrocarbon receptor nuclear translocator. *Proceedings of the National Academy of Sciences of the United States of America* 95: 2844-9

Preibisch S, Saalfeld S, Tomancak P (2009) Globally optimal stitching of tiled 3D microscopic image acquisitions. *Bioinformatics* 25: 1463-5
Qadota H, Inoue M, Hikita T, Koppen M, Hardin JD, Amano M, Moerman DG, Kaibuchi K (2007) Establishment of a tissue-specific RNAi system in C. elegans. *Gene* 400: 166-73
Qin H, Powell-Coffman JA (2004) The Caenorhabditis elegans aryl hydrocarbon receptor, AHR-1, regulates neuronal development. *Developmental biology* 270: 64-75
Qin H, Zhai Z, Powell-Coffman JA (2006) The Caenorhabditis elegans AHR-1 transcription complex controls expression of soluble guanylate cyclase genes in the URX neurons and regulates aggregation behavior. *Developmental biology* 298: 606-15
Rannug A, Rannug U, Rosenkranz HS, Winqvist L, Westerholm R, Agurell E, Grafstrom AK (1987) Certain photooxidized derivatives of tryptophan bind with very high affinity to the Ah receptor and are likely to be endogenous signal substances. *J Biol Chem* 262: 15422-7
Reinke SN, Hu X, Sykes BD, Lemire BD (2010) Caenorhabditis elegans diet significantly affects metabolic profile, mitochondrial DNA levels, lifespan and brood size. *Molecular genetics and metabolism* 100: 274-82
Rieckher M, Bujarrabal A, Doll MA, Soltanmohammadi N, Schumacher B (2018) A simple answer to complex questions: Caenorhabditis elegans as an experimental model for examining the DNA damage response and disease genes. *J Cell Physiol* 233: 2781-2790
Rinaldi AL, Morse MA, Fields HW, Rothas DA, Pei P, Rodrigo KA, Renner RJ, Mallery SR (2002) Curcumin activates the aryl hydrocarbon receptor yet significantly inhibits (-)-benzo(a)pyrene-7R-trans-7,8-dihydrodiol bioactivation in oral squamous cell carcinoma cells and oral mucosa. *Cancer research* 62: 5451-6
Sakakibara H, Nakagawa S, Wakameda H, Nakagiri Y, Kamata K, Das SK, Tsuji T, Kanazawa K (2005) Effects of Japanese kelp (kombu) on life span of benzo[a]pyrene-fed mice. *J Nutr Sci Vitaminol (Tokyo)* 51: 369-73
Schiavi A, Maglioni S, Palikaras K, Shaik A, Strappazzon F, Brinkmann V, Torgovnick A, Castelein N, De Henau S, Braeckman BP, Cecconi F, Tavernarakis N, Ventura N (2015) Iron-Starvation-Induced Mitophagy Mediates Lifespan Extension upon Mitochondrial Stress in C. elegans. *Current biology : CB* 25: 1810-22
Schindelin J, Arganda-Carreras I, Frise E, Kaynig V, Longair M, Pietzsch T, Preibisch S, Rueden C, Saalfeld S, Schmid B, Tinevez JY, White DJ, Hartenstein V, Eliceiri K, Tomancak P, Cardona A (2012) Fiji: an open-source platform for biological-image analysis. *Nature methods* 9: 676-82
Schmitz C, Kinge P, Hutter H (2007) Axon guidance genes identified in a large-scale RNAi screen using the RNAi-hypersensitive Caenorhabditis elegans strain nre-1(hd20) lin-15b(hd126). *Proceedings of the National Academy of Sciences of the United States of America* 104: 834-9
Shimizu Y, Nakatsuru Y, Ichinose M, Takahashi Y, Kume H, Mimura J, Fujii-Kuriyama Y, Ishikawa T (2000) Benzo[a]pyrene carcinogenicity is lost in mice lacking the aryl hydrocarbon receptor. *Proceedings of the National Academy of Sciences of the United States of America* 97: 779-82
Sijen T, Fleenor J, Simmer F, Thijssen KL, Parrish S, Timmons L, Plasterk RH, Fire A (2001) On the role of RNA amplification in dsRNA-triggered gene silencing. *Cell* 107: 465-76
Smith CJ, O'Brien T, Chatzigeorgiou M, Spencer WC, Feingold-Link E, Husson SJ, Hori S, Mitani S, Gottschalk A, Schafer WR, Miller DM, 3rd (2013) Sensory Neuron Fates Are Distinguished by a Transcriptional Switch that Regulates Dendrite Branch Stabilization. *Neuron* 79: 266-80
Sommer C, Strähle C, Köthe U, Hamprecht FA (2011) lastik: Interactive Learning and Segmentation Toolkit. *Eighth IEEE International Symposium on Biomedical Imaging (ISBI) Proceedings*
Sonowal R, Swimm A, Sahoo A, Luo L, Matsunaga Y, Wu Z, Bhingarde JA, Ejzak EA, Ranawade A, Qadota H, Powell DN, Capaldo CT, Flacker JM, Jones RM, Benian GM, Kalman D (2017) Indoles from commensal bacteria extend healthspan. *Proceedings of the National Academy of Sciences of the United States of America* 114: E7506-E7515
Stiernagle T (2006) Maintenance of C. elegans. *WormBook*: 1-11

Tigges J, Krutmann J, Fritsche E, Haendeler J, Schaal H, Fischer JW, Kalfalah F, Reinke H, Reifenberger G, Stuhler K, Ventura N, Gundermann S, Boukamp P, Boege F (2014) The Hallmarks of Fibroblast Ageing. *Mech Ageing Dev*
Tijsterman M, Okihara KL, Thijssen K, Plasterk RH (2002) PPW-1, a PAZ/PIWI protein required for efficient germline RNAi, is defective in a natural isolate of C. elegans. *Current biology : CB* 12: 1535-40
Timmons L, Fire A (1998) Specific interference by ingested dsRNA. *Nature* 395: 854
Torgovnick A, Schiavi A, Shaik A, Kassahun H, Maglioni S, Rea SL, Johnson TE, Reinhardt HC, Honnen S, Schumacher B, Nilsen H, Ventura N (2018) BRCA1 and BARD1 mediate apoptotic resistance but not longevity upon mitochondrial stress in Caenorhabditis elegans. *EMBO Rep*
van der Goot AT, Zhu W, Vazquez-Manrique RP, Seinstra RI, Dettmer K, Michels H, Farina F, Krijnen J, Melki R, Buijsman RC, Ruiz Silva M, Thijssen KL, Kema IP, Neri C, Oefner PJ, Nollen EA (2012) Delaying aging and the aging-associated decline in protein homeostasis by inhibition of tryptophan degradation. *Proceedings of the National Academy of Sciences of the United States of America* 109: 14912-7
van Ham TJ, Thijssen KL, Breitling R, Hofstra RM, Plasterk RH, Nollen EA (2008) C. elegans model identifies genetic modifiers of alpha-synuclein inclusion formation during aging. *PLoS genetics* 4: e1000027
Williams EG, Mouchiroud L, Frochaux M, Pandey A, Andreux PA, Deplancke B, Auwerx J (2014) An evolutionarily conserved role for the aryl hydrocarbon receptor in the regulation of movement. *PLoS genetics* 10: e1004673
Wu H, Huang C, Taki FA, Zhang Y, Dobbins DL, Li L, Yan H, Pan X (2015) Benzo-alpha-pyrene induced oxidative stress in Caenorhabditis elegans and the potential involvements of microRNA. *Chemosphere* 139: 496-503
Xiao R, Chun L, Ronan EA, Friedman DI, Liu J, Xu XZ (2015) RNAi Interrogation of Dietary Modulation of Development, Metabolism, Behavior, and Aging in C. elegans. *Cell reports* 11: 1123-33
Xue Z, Li D, Yu W, Zhang Q, Hou X, He Y, Kou X (2017) Mechanisms and therapeutic prospects of polyphenols as modulators of the aryl hydrocarbon receptor. *Food Funct* 8: 1414-1437
Yang JS, Nam HJ, Seo M, Han SK, Choi Y, Nam HG, Lee SJ, Kim S (2011) OASIS: online application for the survival analysis of lifespan assays performed in aging research. *PloS one* 6: e23525
Ye J, Coulouris G, Zaretskaya I, Cutcutache I, Rozen S, Madden T (2012) Primer-BLAST: A tool to design target-specific primers for polymerase chain reaction. In BMC Bioinformatics
Yigit E, Batista PJ, Bei Y, Pang KM, Chen CC, Tolia NH, Joshua-Tor L, Mitani S, Simard MJ, Mello CC (2006) Analysis of the C. elegans Argonaute family reveals that distinct Argonautes act sequentially during RNAi. *Cell* 127: 747-57
Yueh MF, Huang YH, Hiller A, Chen S, Nguyen N, Tukey RH (2003) Involvement of the xenobiotic response element (XRE) in Ah receptor-mediated induction of human UDP-glucuronosyltransferase 1A1. *J Biol Chem* 278: 15001-6

Figure legends

Figure 1. Loss of *ahr-1* differentially regulates resistance to stressors. A) Survival in response to heat shock. Curves show the pooled data of 60 worms in 3 independent replicates. Statistical test: Log-Rank test, * significance *vs.* wild-type. **B)** Fertility after heat stress. Shown are the number (left panel) and viability (right panel) of eggs laid from gravid adults treated with heat shock for the indicated time. Mean + SEM of pooled data from 18 worms/condition in 3 independent experiments are shown. **C - D)** Development and fertility in response to the indicated concentration of glucose. Means (+SEM) of 3 independent replicates are shown. N = number of individuals in panel C, 9 individuals were used in panel d. **E – F)** Development and fertility in response to the indicated concentration of iron chelator (BP). Means (+SEM) of 3 and 4 independent replicates are shown. N = number of individuals in panel E, 9 individuals were used in panel F. **G – H**) Development and fertility in response to indicated doses of UVB. Fertility was assessed at a dose of 600 J/m². Means (+SEM) of 3 independent replicates are shown. N = number of individuals in panel G, 9 individuals were used in panel H. **B – H)** Statistical test: 2-way ANOVA with Tukey's multiple comparisons test, * significance *vs.* wild-type, # significance *vs.* control (untreated), p-value < 0.05.

Figure 2. AHR-1 displays evolutionarily conserved functions and affects aging in a diet-dependent manner. A – B) Curcumin extends lifespan in an *ahr-1*-dependent manner. Pooled lifespan/healthspan curves of 290 (wt DMSO) and 300 (all other conditions) worms/condition in 5 independent experiments treated wither with DMSO or 100 µM of curcumin are shown. **C – D)** *ahr-1* is more sensitive to xenobiotic stress. Pooled lifespan/healthspan curves of 120 worms/condition in 2 independent replicates treated with either DMSO or 5 µM BaP from adulthood are shown. **E – F)** *ahr-1* is more sensitive to UVB stress. Pooled lifespan/healthspan curves of 300 (wt control, *ahr-1* control), 180 (wt UVB) and 178 (*ahr-1* UVB) worms/condition in 3 independent replicates either left untreated or treated with 1200 J/m² UVB from adulthood are shown. **G – H)** AHR-1 affects aging in a diet-dependent manner. Pooled lifespan/healthspan curves of 170 (wt OP50) and 180 (all other conditions) worms/condition in 3 independent replicates grown either on HT115 or OP50 are shown. **A – H)** Statistical test: Log-Rank test, # significance *vs.* control/HT115, * significance *vs.* wt, p-value < 0.05.

Figure 3. AHR-1 mutants increase aggregation but extend lifespan in a diet-dependent manner.
A – B) Kaplan Meier curves of polyQ;wt and polyQ;ahr-1 of 180 worms/condition in 3 independent experiments are shown. * p-value < 0.05 *vs.* polyQ;wt, # p-value < 0.05 *vs.* HT115, statistical test: Log-rank test.
C) Representative fluorescence images of 10-days old polyQ;wt and polyQ;ahr-1 on HT115 and OP50.
D) Quantification of aggregates in 10-days old polyQ;wt and polyQ;ahr-1. Mean + 95 % CI of pooled data from 34 (wt HT115), 29 (wt OP50), 26 (*ahr-1* HT115), and 35 (*ahr-1* OP50) worms in 3 independent replicates is shown. Statistical test: One-way ANOVA with Tukey's multiple comparisons test, * p-value < 0.05 *vs.* polyQ;wt, # p-value < 0.05 *vs.* HT115. **E – F)** Kaplan Meier curves of a-syn;wt and a-syn;ahr-1 of 120 worms/condition in 2 independent experiments are shown. * p-value < 0.05 *vs.* a-syn;wt, # p-value < 0.05 *vs.* HT115, statistical test: Log-rank test. **G)** Representative fluorescence images of the head muscles of 7-days old a-syn;wt and a-syn;ahr-1 on HT115 and OP50. **H)** Quantification of aggregates in 7- days old a-syn;wt and a-syn;ahr-1. Mean + 95 % CI of pooled data from 77 (wt HT115), 82 (wt OP50), 88 (*ahr-1* HT115), and 92 (*ahr-1* OP50) worms in 3 independent replicates is shown. Statistical test: One-way ANOVA with Tukey's multiple comparisons test, * p-value < 0.05 *vs.* a-syn;wt, # p-value < 0.05 *vs.* HT115.

Figure 4. At 25 °C, *ahr-1(ju145)* is short-lived and loses its protection against the toxicity of polyQ$_{40}$ aggregates. A – B) Kaplan Meier curves of wild-type and *ahr-1(ju145)* at 25 °C. Pooled data of 180

worms/condition in 3 independent replicates are shown. * p-value < 0.05 *vs.* wt, # p-value < 0.05 *vs.* HT115, statistical test: Log-rank test. **C – D)** Kaplan Meier curves of polyQ;wt and polyQ;ahr-1. Worms were grown at 25 °C from day 3 (indicated by arrowhead). Pooled data of 150 worms/condition in 3 independent replicates are shown. * p-value < 0.05 *vs.* wt, # p-value < 0.05 *vs.* HT115, statistical test: Log-rank test. **E)** Representative fluorescence images of 10-days old polyQ;wt and polyQ;ahr-1 grown at 25 °C from day 3. **F)** Quantification of aggregates in 10-days old polyQ;wt and polyQ;ahr-1 grown at 25 °C from day 3. Mean + 95 % CI of pooled data from 21 (wt HT115), 19 (wt OP50), 20 (*ahr-1* HT115) and 19 (*ahr-1* OP50) worms/condition in 2 independent replicates are shown. * p-value < 0.05 *vs.* wt, statistical test: One-way ANOVA with Tukey's multiple comparisons test.

Figure 5. Metabolically active bacteria are required for the differences in lifespan between wild-type and *ahr-1* on HT115. A – C) Survival upon heat stress in 7-days old wild-type and *ahr-1(ju145)* feeding on either HT115 or OP50. Pooled data of 60 worms/condition in 3 independent experiments are shown. * p-value < 0.05 *vs.* wt, # p-value < 0.05 *vs.* HT115, statistical test: Log-rank test. **A)** Living bacteria were used as a food source. **B)** Bacteria were killed by UVB irradiation before seeding to the NGM. **C)** Bacteria had grown on the NGM for 2 days before being killed by UVB irradiation. **D)** Kaplan Meier curves of wild-type and *ahr-1(ju145)* on UVB-killed bacteria. Pooled data of 120 (wt HT115, *ahr-1* HT115, *ahr-1* OP50) and 110 (wt OP50) worms in 2 independent experiments are shown. * p-value < 0.05 *vs.* wt, # p-value < 0.05 *vs.* HT115, statistical test: Log-rank test. **E – F)** Heat stress survival after tryptophan supplementation with indicated concentrations of tryptophan. Survival curves of 7-days old worms feeding on HT115 supplemented with tryptophan are shown. The curves show pooled data from or 40 worms/condition in 2 independent replicates (1.25 mg trp) or 60 worms/condition in 3 independent experiments (2.5 mg trp). * p-value < 0.05 *vs.* wt, # p-value < 0.05 *vs.* HT115, statistical test: Log-rank test. **G)** Positive ESI MS analysis. The HT115 BPC after the subtraction of the OP50 BPC is shown. Masses in peak 2 are shown as inset.

Tables and their legends

Table 1. Survival analysis upon tissue-specific *ahr-1* RNAi. Mean life- and healthspans +/- SEM of pooled data are shown. The L4440 plasmid was used as a negative control. Statistical analysis was performed between *ahr-1* and control RNAi using Log-rank test. The number of worms is specified as N, while the number of replicates is specified as n.

Condition	***Genotype***	***Description***	***Lifespan and healthspan (days)***	***N***	***n***	***P-value***
N2 con	wild-type	wild-type	19.88 ± 0.29 16.00 ± 0.25	280	5	
N2 *ahr-1*			19.46 ± 0.29 15.33 ± 0.25	264	5	0.14 0.04
NR222 con	*rde-1(ne219); kzIs9 [lin-26p::nls::GFP + lin-26p::rde-1) + rol-6(su1006)]*	hypodermis-specific RNAi (Qadota et al., 2007)	19.07 ± 0.34 15.12 ± 0.26	120	2	
NR222 *ahr-1*			18.78 ± 0.30 15.21 ± 0.29	120	2	0.23 0.65
NL2098 con	*rrf-1(pk1417)*	germline-specific RNAi (Kumsta & Hansen, 2012, Sijen et al., 2001)	18.26 ± 0.45 14.16 ± 0.34	120	2	
NL2098 *ahr-1*			18.24 ± 0.43 13.98 ± 0.34	120	2	0.83 0.89
NL2550 con	*ppw-1(pk2505)*	RNAi only in somatic tissues (Tijsterman et al., 2002)	19.51 ± 0.59 15.92 ± 0.53	120	2	
NL2550 *ahr-1*			18.78 ± 0.46 15.25 ± 0.40	120	2	0.11 0.19
WM118 con	*rde-1(ne300); neIs9 [myo-3::HA::RDE-1+ pRF4(rol-6(su1006)]*	muscle-specific RNAi (Yigit et al., 2006)	15.49 ± 0.45 11.91 ± 0.29	120	2	
WM118 *ahr-1*			15.40 ± 0.45 11.44 ± 0.29	120	2	0.92 0.27
VP303 con	*rde-1(ne219); kbIs7 [nhx-2p::rde-1 + rol-6(su1006)]*	intestine-specific RNAi (Espelt et al., 2005)	18.68 ± 0.41 16.52 ± 0.33	120	2	
VP303 *ahr-1*			18.50 ± 0.37 16.78 ± 0.32	120	2	0.47 0.72
TU3401 con	*sid-1(pk3321); uIs69[myo-2p::mCherry + unc-119p::sid-1]*	nervous system specific RNAi (Calixto et al., 2010)	16.48 ± 0.31 12.47 ± 0.23	180	3	
TU3401 *ahr-1*			17.23 ± 0.32 13.03 ± 0.24	180	3	0.09 0.11
TU3311 con	*uIs60[Punc119::YFP; Punc119::sid-1]*	RNAi enhanced in the nervous system (Calixto et al., 2010)	19.99 ± 0.44 15.87 ± 0.37	180	3	
TU3311 *ahr-1*			17.50 ± 0.43 14.11 ± 0.37	180	3	0.001 0.003

Expanded view figure legends

Figure EV1. AHR-1 regulates genes involved in xenobiotic stress response. A) Quantification of *cyp-35A2p::GFP* expression in worms treated with control or *ahr-1* RNAi. Mean + 95 % CI of pooled data from 3 independent experiments with 43 worms are shown. **B)** Quantification of *cyp-37A1p::GFP* expression in worms treated with control or *ahr-1* RNAi. Mean + 95 % CI of pooled data from 2 independent experiments with 38 (con RNAi) and 26 (*ahr-1* RNAi) worms are shown. **C)** Quantification of *cyp-35B1p::GFP* expression in worms treated with control or *ahr-1* RNAi (left panel) or worms with either wildtype *ahr-1* or the *ju145* allele (right panel). Mean + 95 % CI of pooled data from 60 (con RNAi), 40 (*ahr-1* RNAi), 52 (wt), and 63 (*ahr-1*) worms in 3 independent experiments are shown. **D)** Quantification of *ugt-29p::GFP* expression in *ahr-1*-depleted worms. Mean + 95 % CI of pooled data from 3 independent experiments are shown. Number of worms 44 (con RNAi), 36 (*ahr-1* RNAi) [left panel], 34 (wt), 40 (ahr-1) [right panel]. **E)** Quantification of *gst-4p::GFP* expression in worms treated with control or *ahr-1* RNAi (left panel) or worms with either wildtype *ahr-1* or the *ju145* allele (right panel). Mean + 95 % CI of pooled data from 27 (con RNAi), 29 (*ahr-1* RNAi), 27 (wt), and 19 (*ahr-1*) worms in 2 independent experiments are shown. **F)** *ahr-1* depletion via RNAi does not affect the lifespan of N2. Kaplan Meier curves of control (L4440) or *ahr-1* RNAi treated worms. Pooled data of 280 (N2 L4440) and 264 (N2 ahr-1) worms/condition in 5 independent replicates are shown. * p-value < 0.05 *vs.* wt, statistical test: Log-rank test. **G)** *ahr-1* depletion via RNAi shortens the lifespan in a strain with enhanced RNAi in the nervous system (TU3311). Kaplan Meier curves of control (L4440) or *ahr-1* RNAi treated worms. Pooled data of 180 worms/condition in 3 independent replicates are shown. * p-value < 0.05 *vs.* wt, statistical test: Log-rank test.

Figure EV2. *Cyp-13B1* expression is increased by curcumin in an *ahr-1*-dependent manner. A) Fertility over time in response to 100 µM of curcumin. Mean + SEM of 6 worms/condition in 2 independent experiments are shown. * p-value < 0.05 *vs.* wt, # p-value < 0.05 *vs.* DMSO, statistical test: 2-way ANOVA with Tukey's multiple comparisons test. **B)** Expression of *cyp* genes in DMSO-treated *ahr-1* relative to DMSO-treated wild-type. **C)** Expression of *cyp* genes in curcumin-treated wild-type relative to DMSO-treated wild-type. **D)** Expression of *cyp* genes in curcumin-treated *ahr-1* mutants relative to DMSO-treated *ahr-1* mutants. Mean + SEM is shown in panels B - D. * p-value < 0.05 *vs.* wt, # p-value < 0.05 *vs.* DMSO, statistical test: Two-way ANOVA with Tukey's multiple comparisons test.

Figure EV3. Aging is influenced by the bacterial diet in the *ahr-1* mutant. A) Development of wild-type and *ahr-1* on indicated doses of BaP. Pooled data of 3 independent experiments are shown, the number of individuals is presented as N. Statistical test: 2-Way ANOVA with Tukey's multiple comparisons test, no statistical differences were observed. **B)** *cyp-35B1p::GFP* induction in response to 5 µM of BaP. Mean + 95 % CI of pooled data of 58 (wt DMSO), 51 (wt BaP), 53 (*ahr-1* DMSO), and 65 (*ahr-1* BaP) in 3 independent experiments are shown. * p-value < 0.05 *vs*. wt, # p-value < 0.05 *vs.* DMSO, statistical test: One-way ANOVA with Tukey's multiple comparisons test. **C)** UVB irradiation and *ahr-1* loss of function induce apoptosis. Mean + 95 % CI of pooled data of 39 (wt con, *ahr-1* UVB) and 38 (wt UVB, *ahr-1* con) worms in 3 independent experiments are shown. Statistical test: 2-Way ANOVA with Tukey's multiple comparisons test, * p-value < 0.05 *vs*. wt, # p-value < 0.05 *vs.* con. **D)** *cyp-35B1p::GFP* induction in response to UVB irradiation. Mean + 95 % CI of pooled data of 34 (wt con), 37 (wt UVB), 28 (*ahr-1* con), and 35 (*ahr-1* UVB) worms in 2 independent experiments are shown. * p-value < 0.05 *vs*. wt, # p-value < 0.05 *vs.* control, statistical test: One-way ANOVA with Tukey's multiple comparisons test. **E)** Heat shock resistance of wild-type and *ahr-1* feeding on HT115 or OP50. Mean survival times + SEM of 3 independent experiments are shown, the number of individuals is presented as N. Statistical test: Two-way

ANOVA with Tukey's multiple comparisons test. * p-value < 0.05 *vs.* wt, # p-value < 0.05 *vs.* HT115, **F)** *cyp-35B1p::GFP* expression of worms feeding on HT115 or OP50. Mean + 95 % CI of pooled data of 37 (wt HT115), 27 (wt OP50), 44 (*ahr-1* HT115), and 19 (*ahr-1* OP50) in 2 independent experiments are shown. * p-value < 0.05 *vs*. wt, # p-value < 0.05 *vs.* HT115, statistical test: One-way ANOVA with Tukey's multiple comparisons test. **G)** Pumping frequencies of pooled data from 3 independent experiments are shown as mean + 95 % CI, the number of individuals is presented as N. * p-value < 0.05 *vs.* wt, # p-value < 0.05 *vs.* HT115, § p-value < 0.05 *vs.* day 3, statistical test: Two-way ANOVA with Tukey's multiple comparisons test. **H)** *ahr-1* mRNA expression in wild-type worms feeding on HT115 or OP50. Pooled data of 3 independent replicates are shown. No statistical significance was observed with the t-test.

Figure EV4. Gene expression changes in response to Ahr modulators. Expression of the strongest up- and down-regulated genes in *ahr-1* vs. wild-type in response to **A)** 100 µM of curcumin, **B)** 1200 J/m² UVB, and **C)** bacteria. Pooled data from 3 independent replicates are shown. Statistical test: 2-Way ANOVA with Tukey's multiple comparisons test, * significance *vs.* wt, # significance *vs.* control.

Figure EV5. AHR-1 does not influence aging in an Alzheimer's disease model. A – B) Kaplan Meier curves of Abeta;wt and Abeta;ahr-1 grown on HT115. Pooled data of 240 (wt) and 236 (ahr-1) worms/condition in 4 independent replicates are shown. * p-value < 0.05 *vs.* wt, statistical test: Log-rank test. **C – D)** Kaplan Meier curves of Abeta;wt and Abeta;ahr-1 grown on OP50. Pooled data of 120 worms/condition in 2 independent replicates are shown. Statistical evaluation with log-rank test did not display significant differences.

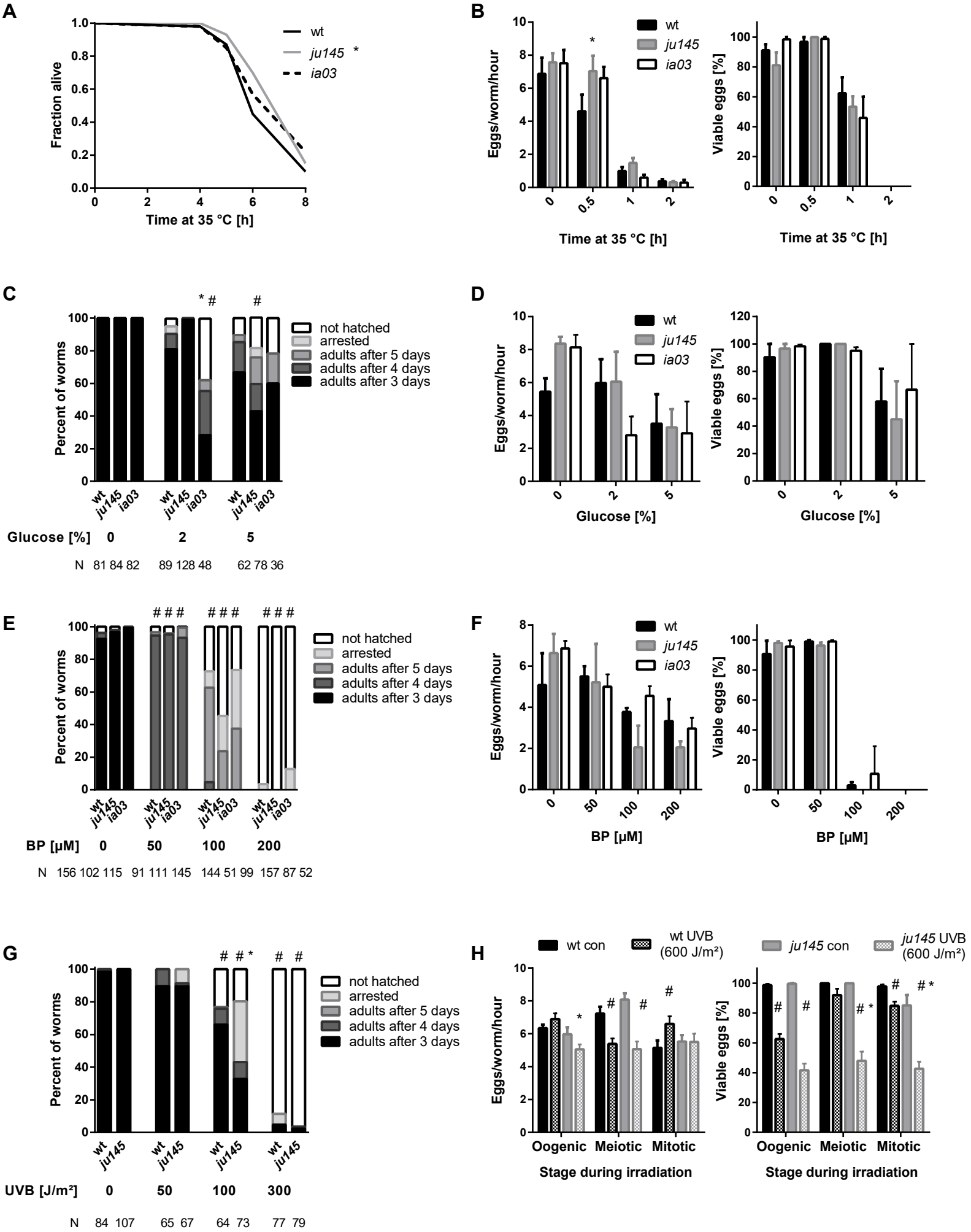
A
Fraction alive
Time at 35 °C [h]
wt
ju145 *
ia03
B
Eggs/worm/hour
Viable eggs [%]
Time at 35 °C [h]
wt
ju145
ia03
C
Percent of worms
not hatched
arrested
adults after 5 days
adults after 4 days
adults after 3 days
Glucose [%] 0 2 5
N 81 84 82 89 128 48 62 78 36
D
Eggs/worm/hour
Viable eggs [%]
Glucose [%]
E
Percent of worms
BP [µM] 0 50 100 200
N 156 102 115 91 111 145 144 51 99 157 87 52
F
Eggs/worm/hour
Viable eggs [%]
BP [µM]
G
Percent of worms
UVB [J/m²] 0 50 100 300
N 84 107 65 67 64 73 77 79
H
wt con
wt UVB (600 J/m²)
ju145 con
ju145 UVB (600 J/m²)
Eggs/worm/hour
Viable eggs [%]
Oogenic
Meiotic
Mitotic
Stage during irradiation

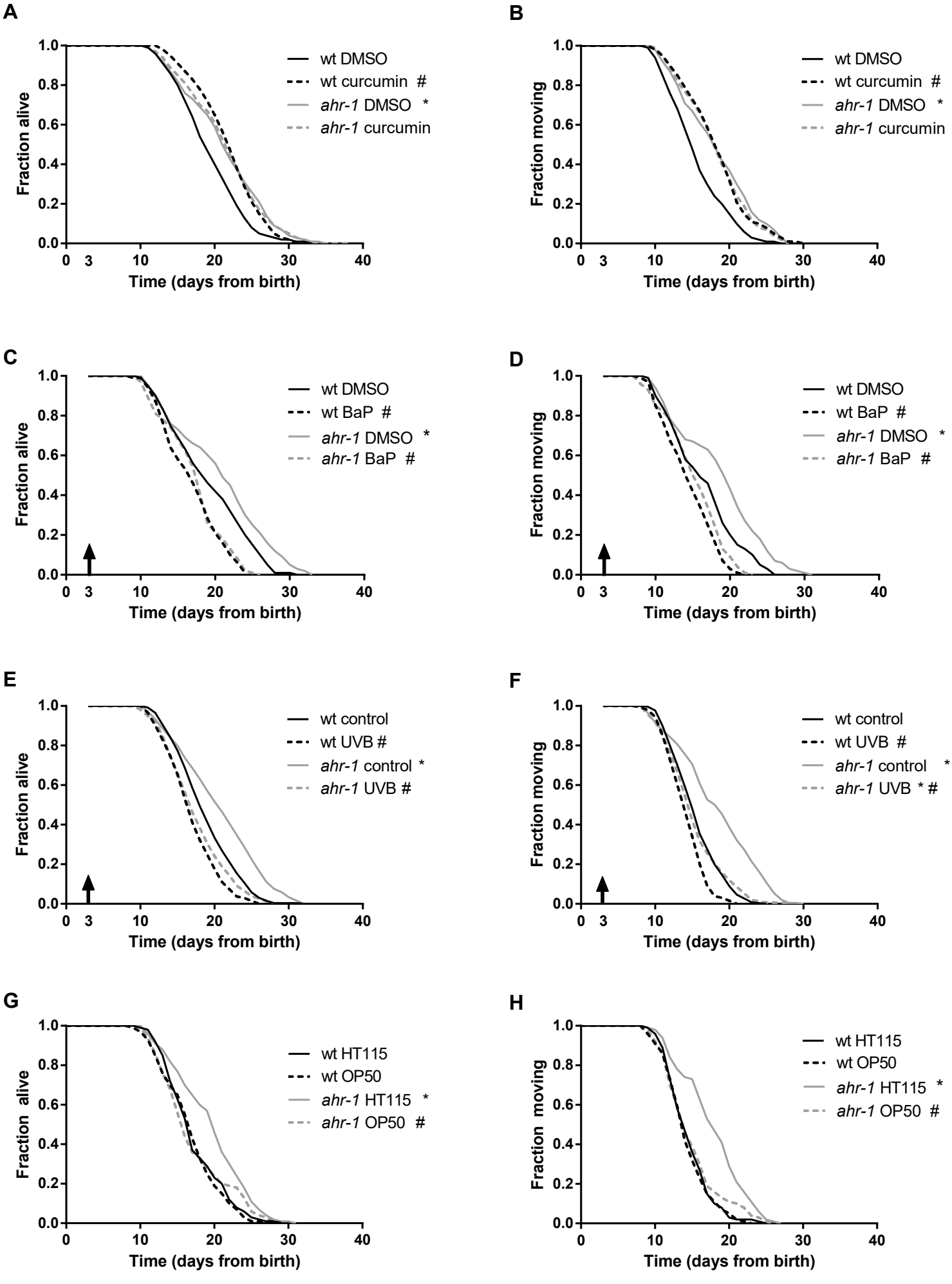
A
Fraction alive
Time (days from birth)
wt DMSO
wt curcumin #
ahr-1 DMSO *
ahr-1 curcumin
B
Fraction moving
Time (days from birth)
wt DMSO
wt curcumin #
ahr-1 DMSO *
ahr-1 curcumin
C
Fraction alive
Time (days from birth)
wt DMSO
wt BaP #
ahr-1 DMSO *
ahr-1 BaP #
D
Fraction moving
Time (days from birth)
wt DMSO
wt BaP #
ahr-1 DMSO *
ahr-1 BaP #
E
Fraction alive
Time (days from birth)
wt control
wt UVB #
ahr-1 control *
ahr-1 UVB #
F
Fraction moving
Time (days from birth)
wt control
wt UVB #
ahr-1 control *
ahr-1 UVB * #
G
Fraction alive
Time (days from birth)
wt HT115
wt OP50
ahr-1 HT115 *
ahr-1 OP50 #
H
Fraction moving
Time (days from birth)
wt HT115
wt OP50
ahr-1 HT115 *
ahr-1 OP50 #

Figure 2

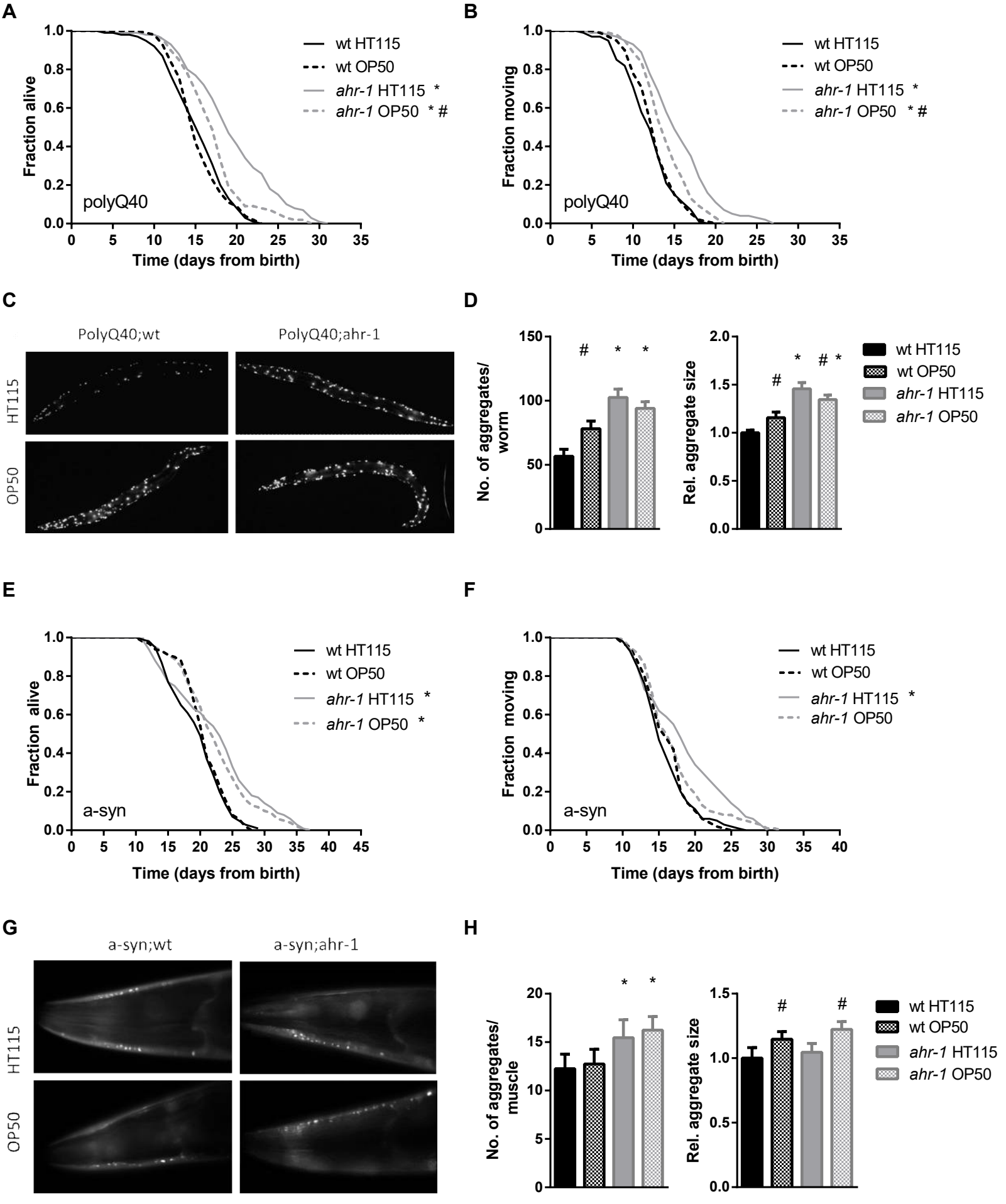
A
Fraction alive
Time (days from birth)
polyQ40
wt HT115
wt OP50
ahr-1 HT115 *
ahr-1 OP50 * #
B
Fraction moving
Time (days from birth)
polyQ40
wt HT115
wt OP50
ahr-1 HT115 *
ahr-1 OP50 * #
C
PolyQ40;wt
PolyQ40;ahr-1
HT115
OP50
D
No. of aggregates/ worm
Rel. aggregate size
wt HT115
wt OP50
ahr-1 HT115
ahr-1 OP50
E
Fraction alive
Time (days from birth)
a-syn
wt HT115
wt OP50
ahr-1 HT115 *
ahr-1 OP50 *
F
Fraction moving
Time (days from birth)
a-syn
wt HT115
wt OP50
ahr-1 HT115 *
ahr-1 OP50
G
a-syn;wt
a-syn;ahr-1
HT115
OP50
H
No. of aggregates/ muscle
Rel. aggregate size
wt HT115
wt OP50
ahr-1 HT115
ahr-1 OP50

Figure 3

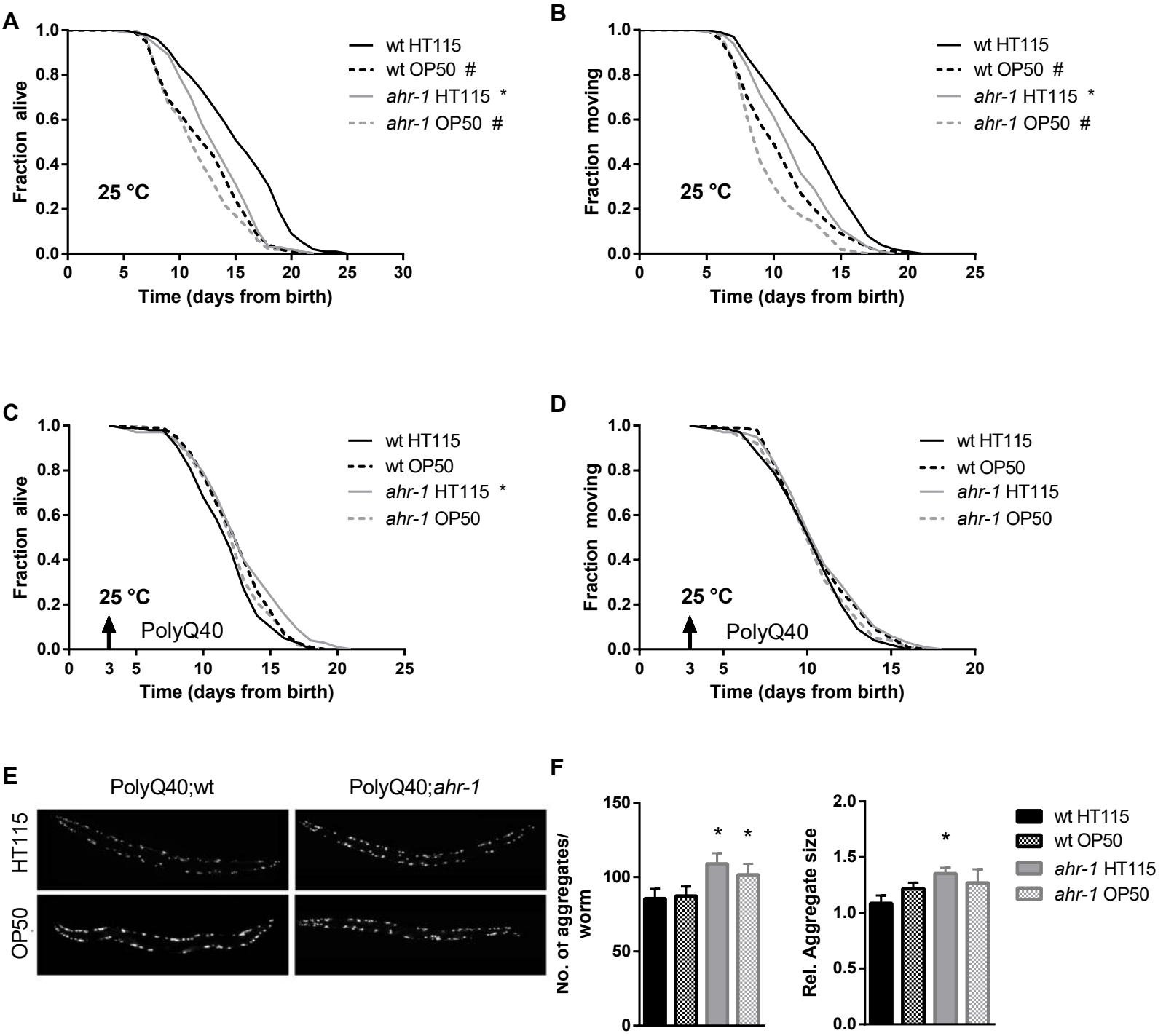
A
Fraction alive
Time (days from birth)
25 °C
wt HT115
wt OP50 #
ahr-1 HT115 *
ahr-1 OP50 #
B
Fraction moving
Time (days from birth)
25 °C
wt HT115
wt OP50 #
ahr-1 HT115 *
ahr-1 OP50 #
C
Fraction alive
Time (days from birth)
25 °C
PolyQ40
wt HT115
wt OP50
ahr-1 HT115 *
ahr-1 OP50
D
Fraction moving
Time (days from birth)
25 °C
PolyQ40
wt HT115
wt OP50
ahr-1 HT115
ahr-1 OP50
E
PolyQ40;wt
PolyQ40;ahr-1
HT115
OP50
F
No. of aggregates/ worm
Rel. Aggregate size
wt HT115
wt OP50
ahr-1 HT115
ahr-1 OP50

Figure 4

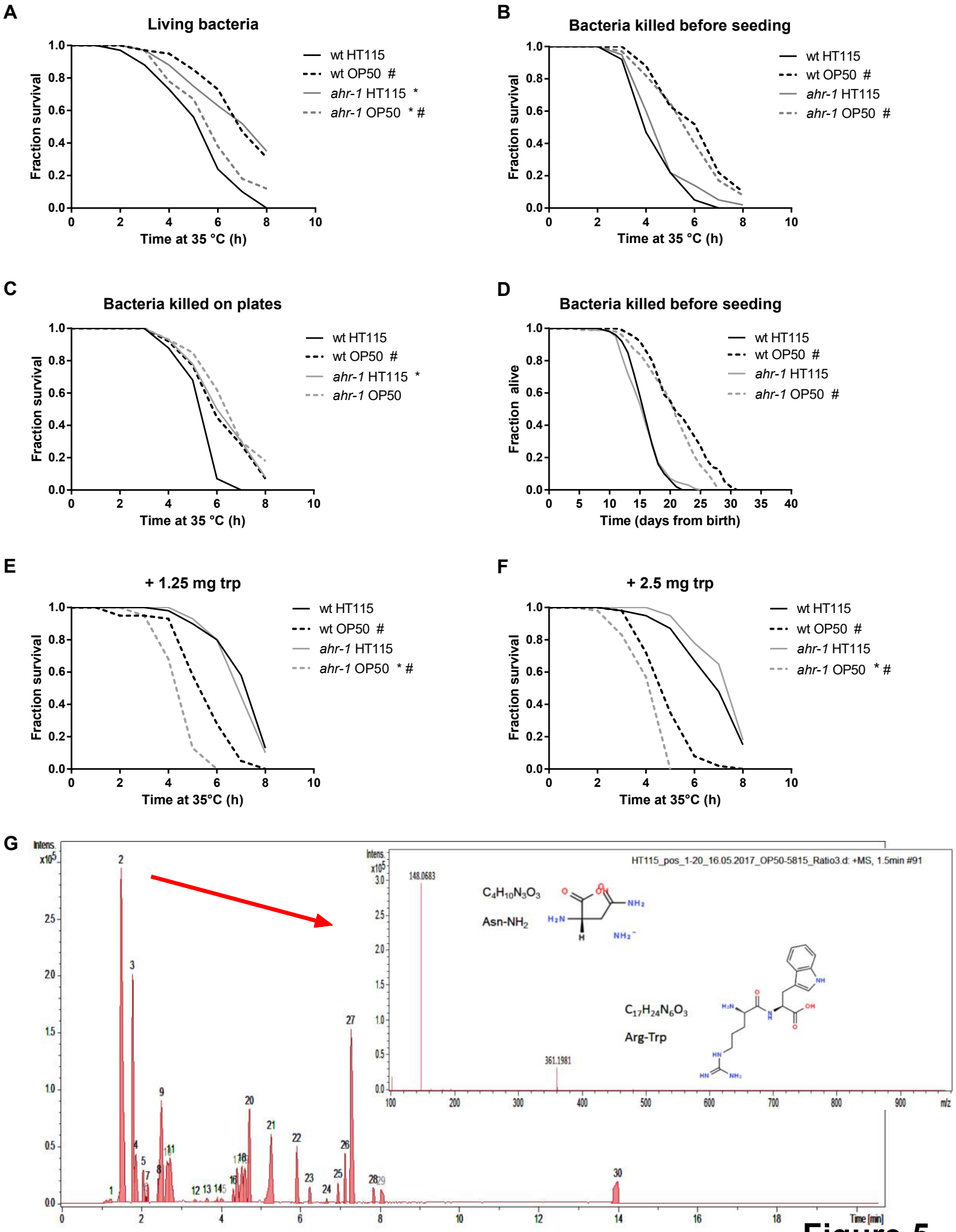
A
Living bacteria
Fraction survival
Time at 35 °C (h)
wt HT115
wt OP50 #
ahr-1 HT115 *
ahr-1 OP50 * #
B
Bacteria killed before seeding
Fraction survival
Time at 35 °C (h)
wt HT115
wt OP50 #
ahr-1 HT115
ahr-1 OP50 #
C
Bacteria killed on plates
Fraction survival
Time at 35 °C (h)
wt HT115
wt OP50 #
ahr-1 HT115 *
ahr-1 OP50
D
Bacteria killed before seeding
Fraction alive
Time (days from birth)
wt HT115
wt OP50 #
ahr-1 HT115
ahr-1 OP50 #
E
+ 1.25 mg trp
Fraction survival
Time at 35°C (h)
wt HT115
wt OP50 #
ahr-1 HT115
ahr-1 OP50 * #
F
+ 2.5 mg trp
Fraction survival
Time at 35°C (h)
wt HT115
wt OP50 #
ahr-1 HT115
ahr-1 OP50 * #
G
Intens.
Time [min]
HT115_pos_1-20_16.05.2017_OP50-5815_Ratio3.d: +MS, 1.5min #91
148.0683
C4H10N3O3
Asn-NH2
361.1981
C17H24N6O3
Arg-Trp
m/z

Figure 5

Appendix

Appendix Tables

Table S1. Relative expression of transgenes in control or *ahr-1* RNAi-treated reporter strains. The relative expression was measured in worms on their first day of adulthood and normalized to control RNAi treated worms in each replicate. N shows the number of worms and n the number of experiments, Statistical test: 2-tailed unpaired t-test.

Strain name	*Gene*	*Rel. expression (mean ± SD)*	*N*	*n*	*p-value*
BC14926	***cyp-14A3***	anterior: 0.97 posterior: 1.05	38 (con) 35 (ahr-1)	3	0.544 0.333
SD1444	***cyp-25A2***	1.07 ± 0.16	38	2	0.067
BC20334	***cyp-29A2***	0.85 ± 0.60	42	2	0.377
cyp-35A2	***cyp-35A2***	anterior: 8.43 ± 11.96 posterior: 1.99 ± 2.14	43 (con) 42 (ahr-1)	3	< 0.001 0.005
cyp-35A3	***cyp-35A3***	1.08 ± 0.09	28 (con) 26 (ahr-1)	2	0.02
CY573	***cyp-35B1***	anterior: 2.60 ± 1.97 posterior: 2.90 ± 2.40	36 (con) 27 (ahr-1) 55 (con) 44 (ahr-1)	2 3	< 0.001 < 0.001
BC15044	***cyp-37A1***	0.66 ± 0.14	46 (con) 26 (ahr-1)	2	< 0.001
CL2166	***gst-4***	1.58 ± 0.37	27 (con) 29 (ahr-1)	2	< 0.001
ugt-29	***ugt-29***	0.96 ± 0.05	44 (con) 36 (ahr-1)	3	0.004

Table S2. List of the most robust over-expressed genes in *ahr-1 vs.* wildtype. Human orthologs were extracted using the BioMart tool (https://parasite.wormbase.org/biomart). Modulators of these genes with potential relevance for AHR-1 activity were selected from WormBase. For log fold change values (logFC) a base of 2 is used.

Gene Name	*human ortholog*	*Molecular function*	*Modulators*	*logFC*	*adj. p-value*
irld-35		unknown	bacterial infection; temperature	1.968	0.0019
clec-209		carbohydrate binding	bacterial infection; aging; quercetin; heat shock	1.882	0.0182
F56A4.2		unknown	aging; bacterial infection; temperature	1.882	0.0182
C01B4.6	GALM	catalytic activity, isomerase activity, carbohydrate binding		1.671	$9.3 * 10^{-9}$
Y19D10A.16	GALM	catalytic activity, isomerase activity, carbohydrate binding		1.671	$9.3 * 10^{-9}$
F56A4.3	GSTP1	unknown	bacterial infection	1.660	0.0013
srd-61		unknown		1.614	0.0001

srd-75		unknown	bacterial infection	1.614	0.0001
C01B4.7		unknown	bacterial infection	1.605	0.0028
Y19D10A.4		transmembrane transporter activity	heat shock; bacterial infection	1.605	0.0028

Table S3. List of the most robust under-expressed genes in *ahr-1* vs. wildtype. Human orthologs were extracted using the BioMart tool (https://parasite.wormbase.org/biomart). Modulators of these genes with potential relevance for AHR-1 activity were selected from WormBase. For log fold change values (logFC) a base of 2 is used.

Gene Name	***human ortholog***	***Molecular function***	***Modulators***	***logFC***	***adj. p-value***
R02F11.1		unknown	bacterial infection; bacterial diet	-2.308	0.0312
hbl-1	ZNF513 ZNF462	RNA polymerase II regulatory region sequence-specific DNA binding, RNA polymerase II transcription factor activity, sequence-specific DNA binding, transcription factor activity, metal ion binding	bacterial infection; quercetin; aging	-2.013	0.0171
atf-2		RNA polymerase II regulatory region DNA binding, transcriptional repressor activity, RNA polymerase II core promoter proximal region sequence-specific binding, transcription factor activity, protein binding	*ahr-1*; bacterial infection; quercetin; aging	-1.958	0.0227
lpr-4		unknown	bacterial infection; quercetin; bacterial diet; indole	-1.834	0.0227
K04H4.2		chitin binding	*ahr-1*; bacterial infection; bacterial diet	-1.831	0.0248
egl-46	INSM1 INSM2	RNA polymerase II transcription factor activity, sequence-specific DNA binding, RNA polymerase II transcription factor binding	bacterial infection; quercetin; aging	-1.823	0.0406
T20F5.4		unknown	bacterial infection; quercetin	-1.803	0.0400
ptr-4	PTCHD3	unknown	resveratrol; bacterial infection; quercetin; bacterial diet; aging	-1.766	0.0162
lpr-5		unknown	bacterial infection; bacterial diet; aging; quercetin;	-1.752	0.0227

			indole		
dyf-7		protein self-association	quercetin; bacterial infection; temperature	-1.743	0.0227

Table S4. *C. elegans* strains used in this study. Strains are sorted alphabetically.

Strain name	***Genotype***
BC14926	*dpy-5(e907); sEx14926[rCes K09A11.4::GFP + pCeh361]*
BC15044	*dpy-5(e907); sEx15044[rCes F01D5.9::GFP + pCeh361]*
BC20306	*cyp-34A9p::GFP*
BC20334	*cyp-29A2p::GFP*
CL2166	*pAF15)gst-4p::GFP::NLS*
CY573	*cyp-35B1p::GFP + gcy-7p::GFP*
cyp35A2	*cyp-35A2p::GFP*
cyp35A3	*cyp-35A3p::GFP*
cyp35A5	*cyp-35A5p::GFP*
cyp33E2	*cyp-33E2p::GFP*
CZ2485	*ahr-1(ju145)*
N2	*wild-type*
NL2098	*rrf-1(pk1417)*
NL2550	*ppw-1(pk2505)*
NR222	*rde-1(ne219); kzIs9[lin-26p::nls::GFP + lin-26p::rde-1 + rol-6(su1006)]*
NV33a	*cyp-35B1p::GFP + gcy-7p::GFP; ahr-1(ju145)*
NV33wt	*cyp-35B1p::GFP + gcy-7p::GFP*

Strain name	***Genotype***
NV35a	*ahr-1(ju145); (pAF15)gst-4p::GFP::NLS*
NV35wt	*pAF15)gst-4p::GFP::NLS*
NV38b	*ahr-1(ju145); unc-54p::Q40::YFP*
NV38wt	*unc-54p::Q40::YFP*
NV41a	*unc-119p::Aβ 1–42; Pmyo-2::YFP; ahr-1(ju145)*
NV41wt	*unc-119p::Aβ 1–42; Pmyo-2::YFP*
NV42a	*unc-54p::alphasynuclein::YFP, ahr-1(ju145)*
NV42wt	*unc-54p::alphasynuclein::YFP*
NV47a	*ugt-29p::GFP; ahr-1(ju145)*
NV47wt	*ugt-29p::GFP*
SD1444	*unc-119(ed3); gaIs237 [cyp-25A2p::his-24::mCherry + unc-119(+)]*
TU3311	*uIs60[unc119p::YFP; unc119p::sid-1]*
TU3401	*sid-1(pk3321); uls69[myo-2p::mCherry + unc-119p::sid-1]*
ugt-29	*ugt-29p::GFP*
VP303	*rde-1(ne300); neIs9 [myo-3::HA::RDE-1+ rol-6(su1006)]*
WM118	*rde-1(ne219); kbIs7 [nhx-2p::rde-1 + rol-6(su1006)]*
ZG24	*ahr-1(ia03)*

Table S5. Primer pairs used in this study to validate genes differentially expressed between *ahr-1(ju145)* and wild-type (Figure S4).

Gene		***Sequence (5‘ – 3‘)***	***Annealing temp. (°C)***	***Efficiency (%)***
clec-209	**F**	TGCTCGGGGAACAACCAAAA	60	88.4
	R	TTGGCTACGAACGATTGATGC		
C01B4.6	**F**	TGGCGATGCGAAAATTGATGTAA	61	83.9
	R	ATCTCCAGAAAGTGCTCGGC		
F56A4.3	**F**	ACGAGGGGAATGAATGGCAA	67	101.4
	R	CCATAGGGACCAATATCCATGAACT		
C01B4.7	**F**	GTTTTGGAATCAGACGCGGG	67	106.6
	R	CAGTGGGGTTCCGTCAAGTT		
hbl-1	**F**	TTGGCACAAAGAGCAAAGCC	58	113.1

Gene		Sequence (5‘ – 3‘)	Annealing temp. (°C)	Efficiency (%)
cyp-13A1	F	GTACAACCTACACAAATCGC	55.5	91.2
	R	TGAATCTCTGGATGAGTTGC		
cyp-13A2	F	GTGGACAAAGAAATATGGCAA	52.7	97.6
	R	ACAAGTGAACTCGTTGTTCT		
cyp-13A3	F	GCCTGAAAGATGGGAATCTG	52.7	100.5
	R	TGCCAGAAGCATCTTTTCTT		
cyp-13A5	F	TGGACAAAAGAATACGGACC	55.0	86.7
	R	CGTAGGTGATGACAGAGTTC		
cyp-13A7	F	GACAAAGAAATACGGACCTG	52.7	93.2
	R	TGCAGTTAATTTTCTCCCGT		
cyp-13A8	F	AGCTCAAGGTTTTAGATGGA	52.7	94.0
	R	CATAAGCTCCTGTGTGCTAT		
cyp-13A10	F	AAGACAGTGCGATGGAATTA	52.0	103.7
	R	TCTCCGAATATCGCTCTGA		
cyp-13A12	F	CTGGGAGCTTTAGCAAATTC	55.0	105.8
	R	TCTCCTGATTCCCATCTTTC		
cyp-13B1	F	GGGCTGTTCCAGTGTTAGTC	52.7	96.2
	R	AACATCGTGAACCTGCTTTA		
cyp-13B2	F	TGAGAATGTATCCAGTTGCC	55.0	98.7
	R	GATTCGAGCCATCTTTCTGG		
cyp-14A1	F	TTCACCAGTTCCCTCCAGAC	59.0	94.4
	R	AGAACGGTGAGCTCGGTAAG		
cyp-14A2	F	AGTCCGGAAGGAAATACTTG	55.0	102.3
	R	CATCTCGGTTTGTATGAGTC		
cyp-14A5	F	ATAGGCACGGCGAGACTACC	52.7	100.1
	R	CAAGTACAGTCTTGTTCAAC		
cyp-25A1	F	TGGCTCTCCTGATTTTAAGC	52.7	84.75
	R	AAGTTTTTCCTTGCGTTCTG		
cyp-25A2	F	CTCTTCTGATTCTCACCTCAA	53.0	93.1
	R	TTTTTCTTTCCGGTCAACGA		
cyp-25A3	F	AGCACTTCTTTCCTTTTCCC	55.0	109.2
	R	TAAACATCTGCAAGTCCCTC		
cyp-25A4	F	CCAGTGTCTTTGATACTTCC	55.0	106.4
	R	ACCCTCTCCAGCACGTCTTC		
cyp-29A2	F	TGCCATAATTCTGGCATATC	52.7	90.3
	R	AGGACCAGGTAGTTTACTTC		
cyp-29A4	F	TTCCAGTGGCTCTTGCATTG	55.5	107.4
	R	CATCTTTCCTCCATAAATCCAG		
cyp-31A2	F	CCGCTGTACTTCTCGCTATG	59.0	84.3
	R	TTCTTCATCTGCTCCGAGGC		
cyp-31A3	F	TACTCCGCCGATCTCGTG	57.5	81.8
	R	TTCTTCCTCTGCTCCGAGGG		
cyp-32A1	F	TCCTAGCTGATGCAGTCGAG	57.0	94.65
	R	CCGTTCTTGGATGACCTTTC		
cyp-32B1	F	AGTTTTTGCATGTTCGGAAG	51.5	97.85
	R	ACCATAACTTCAACACACCA		
cyp-33A1	F	GAAGTTAATATTCAGGAACAT	49.5	100.6
	R	TACGCGAAGTAGACACGAAG		
cyp-33C4	F	AAAATCTTCCCAGACCCCT	54.0	107.25
	R	GAAGACGGTGAGATCTTGTATCTA		
cyp-33C5	F	GTTTGTTTGTTCCTGTTCCA	51.5	92.45
	R	CATATGGAATGTTGCCCATC		
cyp-33C7	F	GAAGATTTGATGAAAGACTGGA	54.0	97.35
	R	CAGAGGTCCAAGCAAGTATT		
	F	[illegible]		

Table S6. Primer pairs used for the assessment of *cyp* gene expression in DMSO and curcumin-treated wild-type and *ahr-1(ju145)* (Figure S2).

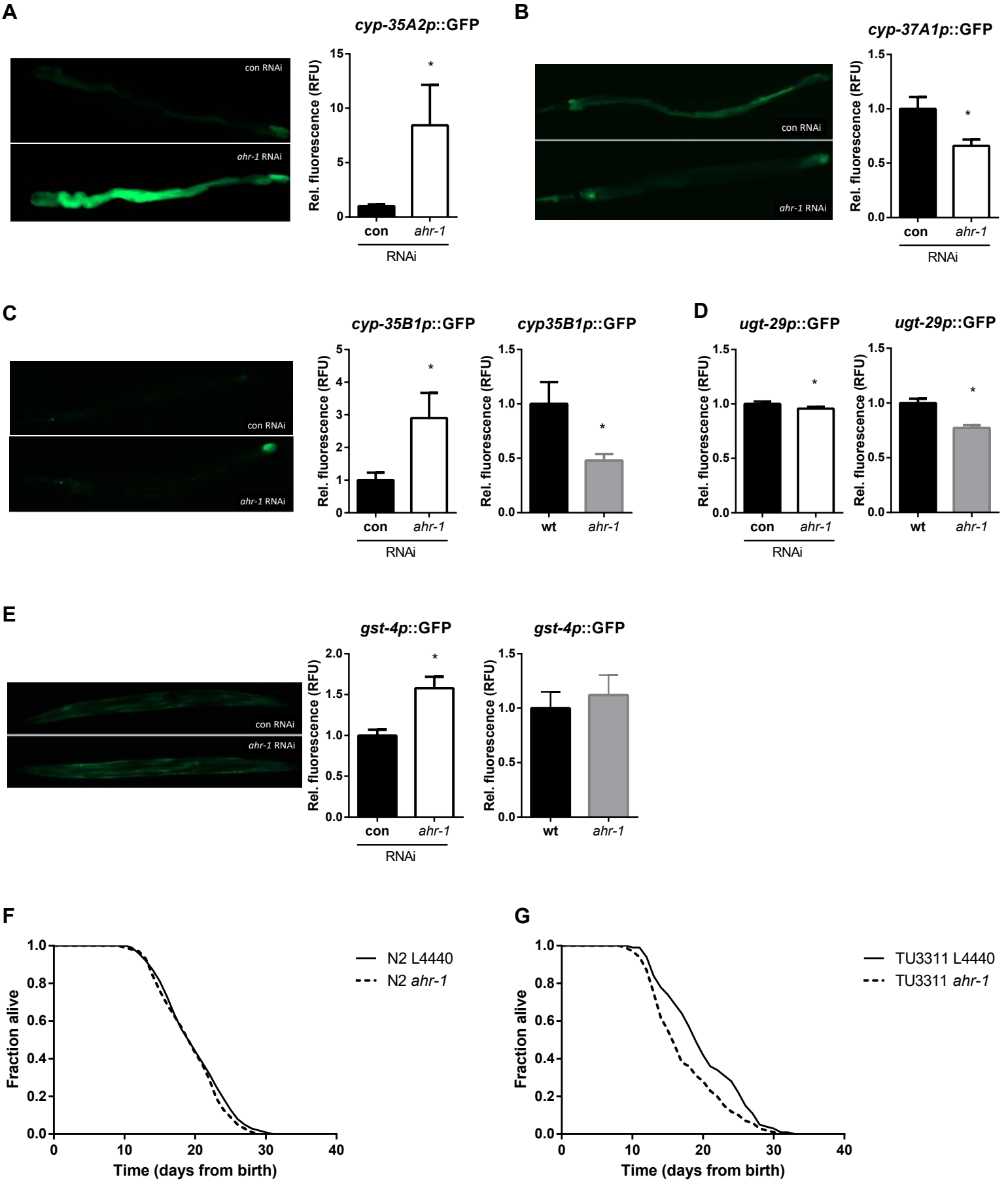
A
cyp-35A2p::GFP
con RNAi
ahr-1 RNAi
Rel. fluorescence (RFU)
con
ahr-1
RNAi
B
cyp-37A1p::GFP
C
cyp-35B1p::GFP
cyp35B1p::GFP
wt
D
ugt-29p::GFP
E
gst-4p::GFP
F
N2 L4440
N2 ahr-1
Fraction alive
Time (days from birth)
G
TU3311 L4440
TU3311 ahr-1

Figure EV1

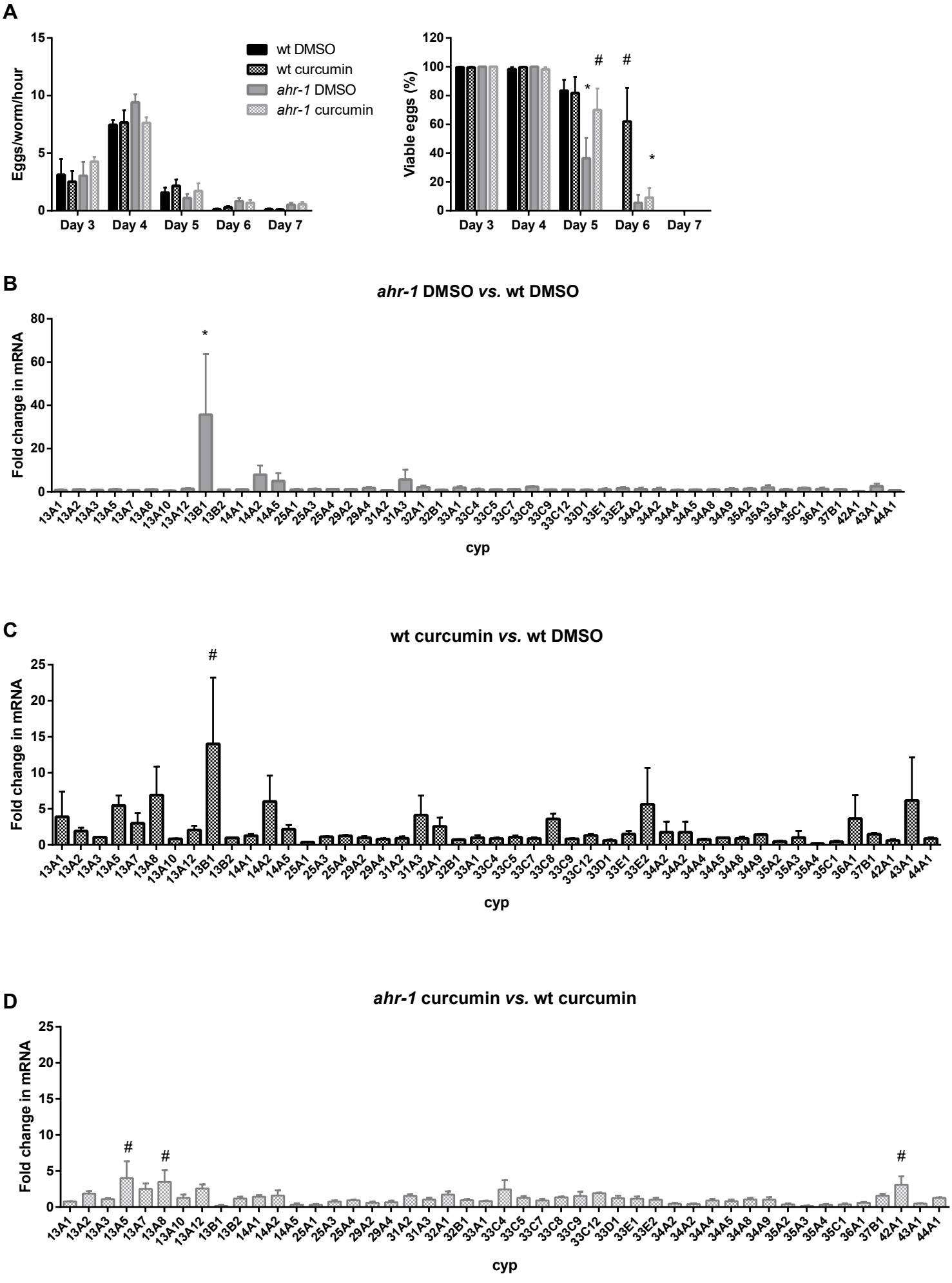
A
Eggs/worm/hour
wt DMSO
wt curcumin
ahr-1 DMSO
ahr-1 curcumin
Day 3
Day 4
Day 5
Day 6
Day 7
Viable eggs (%)
B
ahr-1 DMSO vs. wt DMSO
Fold change in mRNA
cyp
C
wt curcumin vs. wt DMSO
Fold change in mRNA
cyp
D
ahr-1 curcumin vs. wt curcumin
Fold change in mRNA
cyp

Figure EV2

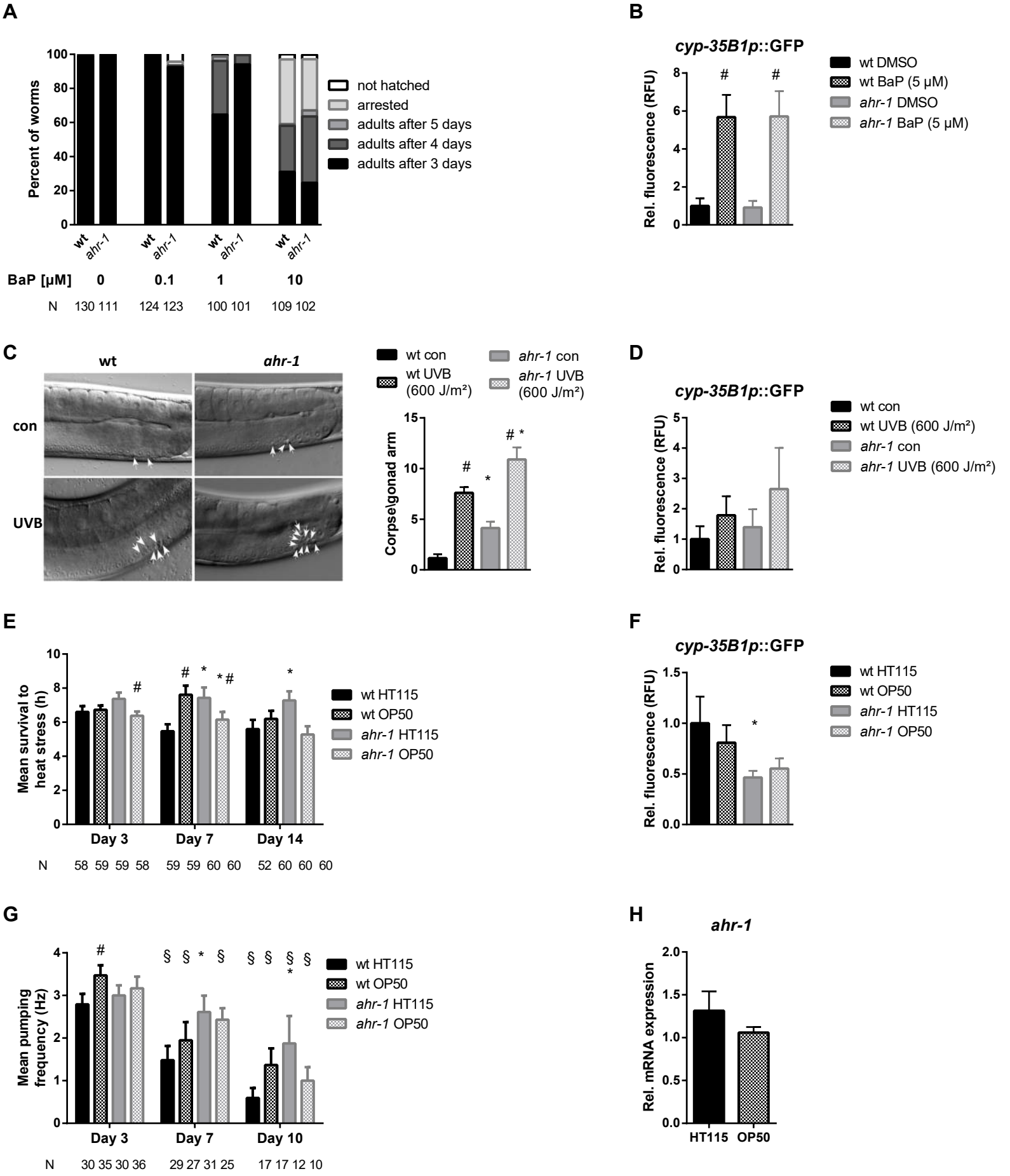
A
Percent of worms
100
80
60
40
20
0
not hatched
arrested
adults after 5 days
adults after 4 days
adults after 3 days
wt
ahr-1
BaP [µM] 0 0.1 1 10
N 130 111 124 123 100 101 109 102
B
cyp-35B1p::GFP
Rel. fluorescence (RFU)
wt DMSO
wt BaP (5 µM)
ahr-1 DMSO
ahr-1 BaP (5 µM)
C
wt
ahr-1
con
UVB
wt con
wt UVB (600 J/m²)
ahr-1 con
ahr-1 UVB (600 J/m²)
Corpse\gonad arm
D
cyp-35B1p::GFP
Rel. fluorescence (RFU)
wt con
wt UVB (600 J/m²)
ahr-1 con
ahr-1 UVB (600 J/m²)
E
Mean survival to heat stress (h)
Day 3
Day 7
Day 14
N 58 59 59 58 59 59 60 60 52 60 60 60
wt HT115
wt OP50
ahr-1 HT115
ahr-1 OP50
F
cyp-35B1p::GFP
Rel. fluorescence (RFU)
wt HT115
wt OP50
ahr-1 HT115
ahr-1 OP50
G
Mean pumping frequency (Hz)
Day 3
Day 7
Day 10
N 30 35 30 36 29 27 31 25 17 17 12 10
wt HT115
wt OP50
ahr-1 HT115
ahr-1 OP50
H
ahr-1
Rel. mRNA expression
HT115
OP50

Figure EV3

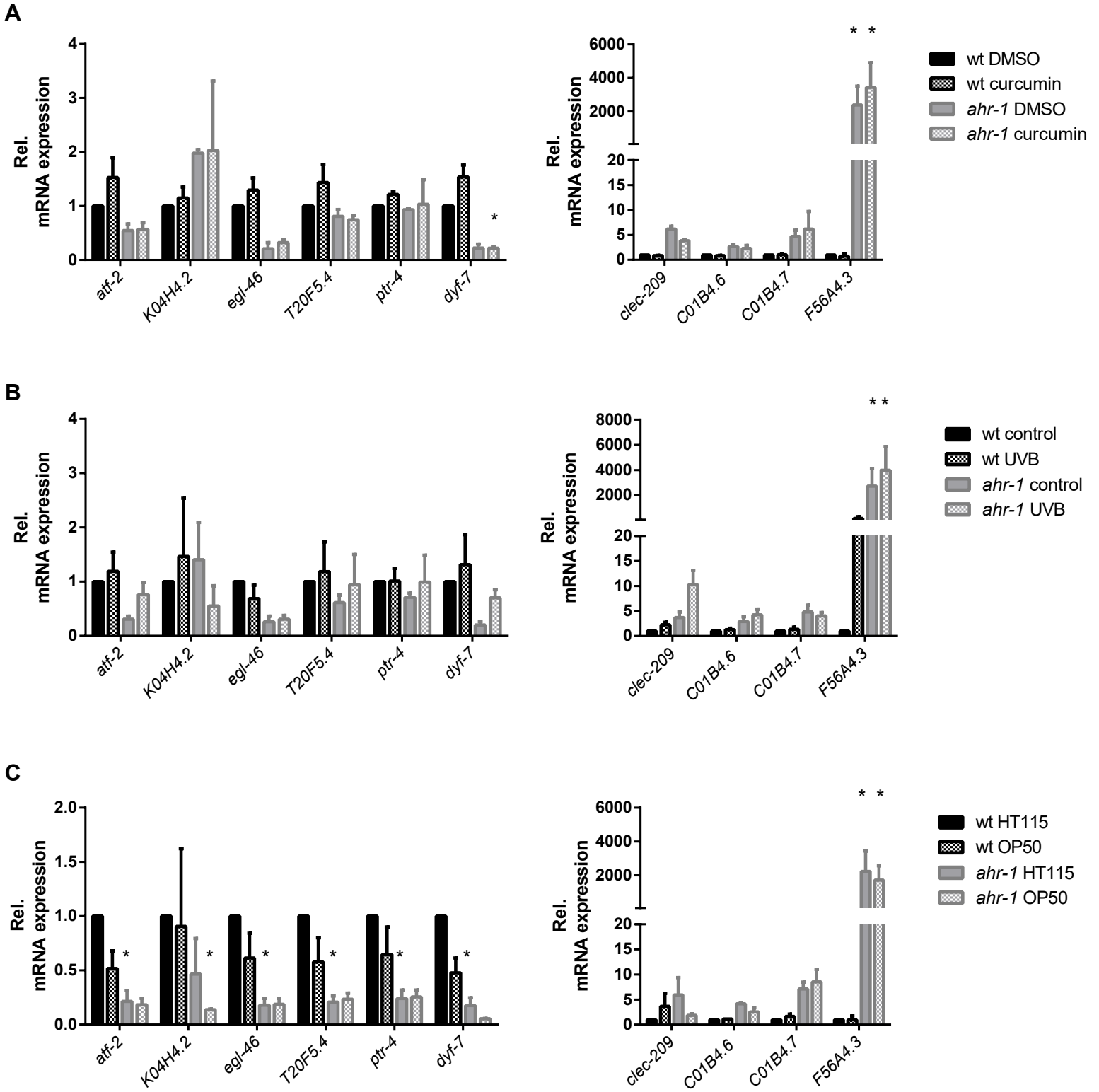
A
Rel. mRNA expression
atf-2
K04H4.2
egl-46
T20F5.4
ptr-4
dyf-7
clec-209
C01B4.6
C01B4.7
F56A4.3
wt DMSO
wt curcumin
ahr-1 DMSO
ahr-1 curcumin
B
wt control
wt UVB
ahr-1 control
ahr-1 UVB
C
wt HT115
wt OP50
ahr-1 HT115
ahr-1 OP50

Figure EV4

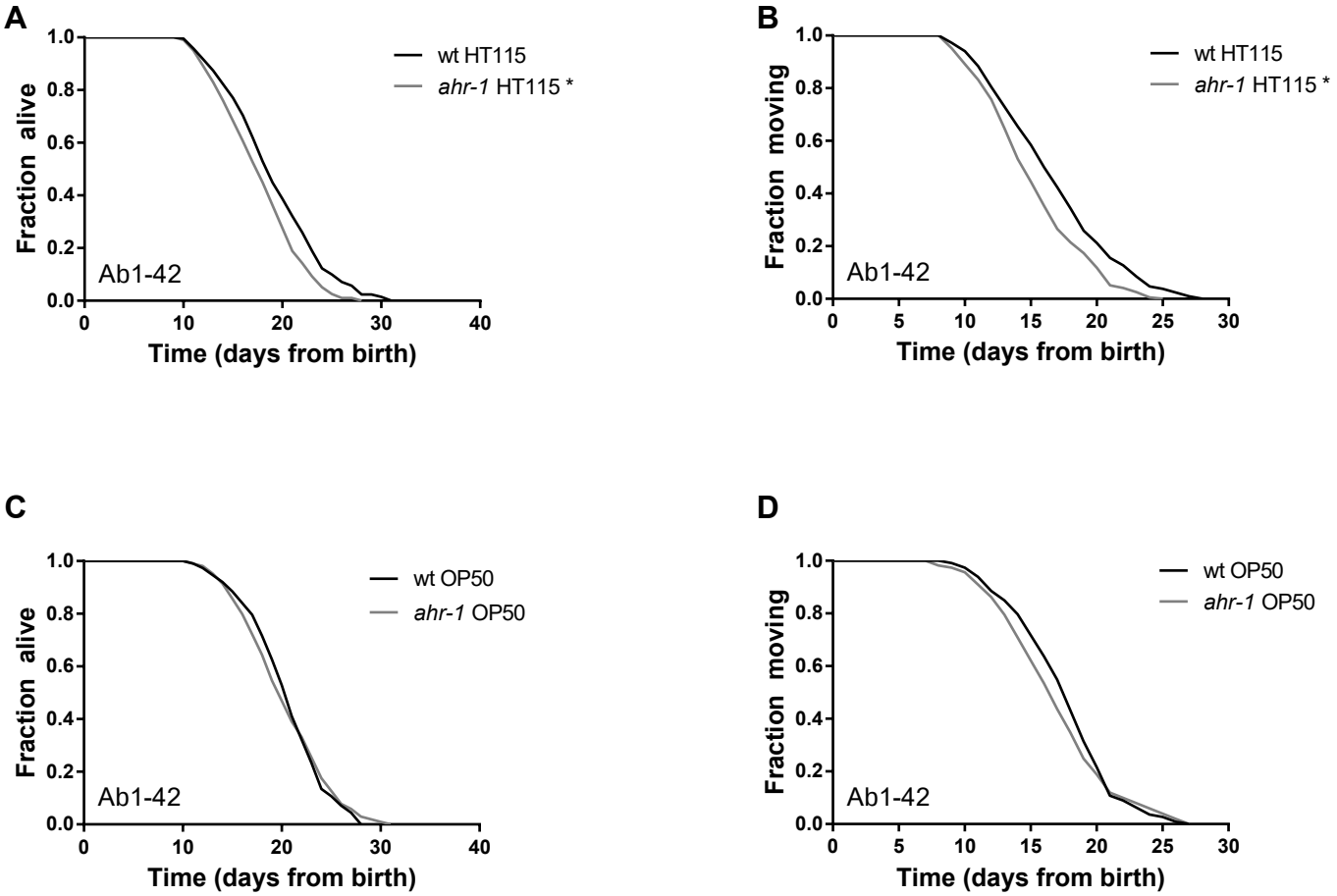
A
Fraction alive
1.0
0.8
0.6
0.4
0.2
0.0
0
10
20
30
40
Time (days from birth)
wt HT115
ahr-1 HT115 *
Ab1-42
B
Fraction moving
1.0
0.8
0.6
0.4
0.2
0.0
0
5
10
15
20
25
30
Time (days from birth)
wt HT115
ahr-1 HT115 *
Ab1-42
C
Fraction alive
1.0
0.8
0.6
0.4
0.2
0.0
0
10
20
30
40
Time (days from birth)
wt OP50
ahr-1 OP50
Ab1-42
D
Fraction moving
1.0
0.8
0.6
0.4
0.2
0.0
0
5
10
15
20
25
30
Time (days from birth)
wt OP50
ahr-1 OP50
Ab1-42

Figure EV5